Journal of Marine Science and Technology

Volume 28 | Issue 3 Article 4

NUMERICAL ANALYSES OF PILE FOUNDATION FOR SUPPORT STRUCTURE OF OFFSHORE WIND TURBINE AT CHANGHUA COAST IN TAIWAN

Der-Guey Lin
Department of Soil and Water Conservation, National Chung Hsing University, Taichung, Taiwan, R.O.C

Sheng-Hsien Wang
Department of Soil and Water Conservation, National Chung Hsing University, Taichung, Taiwan, R.O.C.

Jui-Ching Chou
Department of Civil Engineering, National Chung Hsing University, Taichung, Taiwan, R.O.C, jccchou@nchu.edu.tw

Cheng-Yu Ku
Department of Harbor and River Engineering, National Taiwan Ocean University, Keelung, Taiwan, R.O.C.

Lien-Kwei Chien
Department of Harbor and River Engineering, National Taiwan Ocean University, Keelung, Taiwan, R.O.C.

Recommended Citation

Lin, Der-Guey; Wang, Sheng-Hsien; Chou, Jui-Ching; Ku, Cheng-Yu; and Chien, Lien-Kwei (2020) "NUMERICAL ANALYSES OF PILE FOUNDATION FOR SUPPORT STRUCTURE OF OFFSHORE WIND TURBINE AT CHANGHUA COAST IN TAIWAN," *Journal of Marine Science and Technology*: Vol. 28: Iss. 3, Article 4.
DOI: 10.6119/JMST.202006_28(3).0004
Available at: https://jmstt.ntou.edu.tw/journal/vol28/iss3/4

Journal of Marine Science and Technology, Vol. 28, No. 3, pp. 179-199 (2020)
DOI: 10.6119/JMST.202006_28(3).0004

NUMERICAL ANALYSES OF PILE FOUNDATION FOR SUPPORT STRUCTURE OF OFFSHORE WIND TURBINE AT CHANGHUA COAST IN TAIWAN

Der-Guey Lin[1], Sheng-Hsien Wang[1], Jui-Ching Chou[2]

Cheng-Yu Ku[3], and Lien-Kwei Chien[3]

Key words: group pile foundation, bearing capacity, offshore wind turbine (OWT), *V-H-M* envelopes of bearing capacity.

ABSTRACT

This study investigates the bearing capacities of group pile foundation (jacket foundation) installed on the seabed of offshore wind farm (OWF) at the Changhua coast of Western Taiwan for the jacket support structure of offshore wind turbine (OWT) using three-dimensional (3-D) finite element method (FEM). The jacket foundations are subjected to a combined *V*ertical-*H*orizontal-*M*oment (*V-H-M*) loading for the operational period. The responses of installed group pile foundations are investigated under the combined loading in marine silty sand-low plasticity silt & clay (*SM-ML-CL*) layers determined by 19 offshore boring logs. The validity of numerical procedures was verified by a large-scale lateral loading test of steel tubular model pile in laboratory. A systematic parametric study was performed to investigate the effects of the pile length *L*, pile diameter *D*, and pile spacing *S* on the ultimate bearing (or load) capacity behavior of the foundation. The effect of pile length is significant on the vertical bearing capacity (V_{ult}) whereas pile diameter and pile spacing on the ultimate horizontal and moment loads bearing capacities (H_{ult} and M_{ult}). The normalized *V-H* and *V-H-M* failure envelopes of bearing capacity for the jacket foundations subjected to combined loadings can be expressed as functions of *L*, *D*, and *S* and fitted by elliptical shape curves. The *V-H-M* failure envelopes and approximated expressions are proposed to evaluate the mechanical stability of the group pile foundations for the jacket support structure of OWT under the combined loading condition.

I. INTRODUCTION

With the rapid development of wind power technology, the offshore wind electric power generation has become the international focus of renewable energy. Sweden installed the first offshore wind turbine (OWT) in the world near the Nogersund at Baltic Sea in 1990. At present, the development of offshore wind farm (OWF) in the global mainly concentrates on the European countries in the North Sea and Baltic Sea such as United Kingdom, Denmark, Netherlands, Germany, Belgium and Sweden. In Asian, China, India, Japan and Taiwan are assessed as areas with potential for the development of offshore wind electric power generation (Siegfriedsen et al., 2003). Within the next decade, the development and utilization of offshore wind energy will grow into an important policy of renewable energy to Taiwan Government. Currently, in Taiwan, the western coast is the most suitable area for the development of OWF, accordingly this study selects the Changhua coastal wind farm as the research site. However, it must be pointed out that the relevant specifications and development experiences of the foundation design for OWT in European countries are difficult to apply directly to Taiwan due to the very soft marine soil strata at the OWF of western coast. The foundation design for the support structure of OWT has enormous influences on its engineering safety and the costs of foundation engineering generally account for about 25 to 30 % of the design and construction costs of OWT (Lesny, 2008). Therefore, to achieve a safe and economical design of pile foundation for OWT, it must be performed in accordance with the specific geological conditions of seabed in Taiwan.

The commonly used foundation systems supporting OWT are introduced as followed. Monopiles are single open-ended

Paper submitted 10/24/19; revised 11/26/19; accepted 12/30/19. Corresponding Author: Jui-Ching Chou (e-mail:jccchou@nchu.edu.tw)
[1] Department of Soil and Water Conservation, National Chung Hsing University, Taichung, Taiwan, R.O.C.
[2] Department of Civil Engineering, National Chung Hsing University, Taichung, Taiwan, R.O.C.
[3] Department of Harbor and River Engineering, National Taiwan Ocean University, Keelung, Taiwan, R.O.C.

Table 1. Comparison on investigating various potential foundations concept for supporting OWT using 3-D FEM.

Researcher	Foundation Type (Numerical tool)	Summary of Investigation using 3-D FEM
Abdel-Rahman and Achmus (2005)	Monopole (ABAQUS^{3D})	(1) The *p*-*y* curve method given in API (2000) underestimated pile deformations compared with numerical results. (2) For a large-diameter pile the shearing resistance in the pile tip area may play an important role compared to a small-diameter pile.
Aliasger and Gopal (2012)	Monopole (ABAQUS^{3D})	(1) Bending moment and shear force in a small-diameter pile are concentrated along the upper portion of the pile only whereas in a large-diameter monopile are mobilized along the entire length of the pile. (2) A monopile deforms primarily through rigid body rotation whereas a conventional small-diameter pile is flexible and deforms by bending.
Murphy et al. (2018)	Monopole (PLAXIS^{3D})	(1) As the (*L*/*D*) ratio of the piles reduced, the second order resistance components make a larger contribution to the ultimate moment resistance of the piles. (*L*=embedded pile length, *D*=pile diameter)
Zhan and Liu (2010)	Suction bucket (ABAQUS^{3D})	(1) Horizontal capacity factor decreases with increasing aspect ratio (*L*/*D*). (*L*=embedded bucket length, *D*=bucket diameter). The torsional load has significant effect on the vertical capacity whereas slight effect on the horizontal capacity (2) The locus expands with increasing torsional load and can be represented by elliptic curve.
Britta Bienen et al. (2012)	Hybrid bucket (ABAQUS^{3D})	(1) A hybrid skirted foundation with additional internal skirts which exceed the length of the external skirts is found to provide significantly increased horizontal capacity and moment capacity as well. (2) The potential of this foundation concept to be an economical foundation alternative compared with a large bucket foundation.
Achmus et al. (2013)	Monopod bucket (ABAQUS^{3D})	(1) The ultimate capacity of a bucket in very to medium dense sand is dependent on the bucket geometry (skirt length and bucket diameter), the relative density of the sand and load eccentricity.
Kim et al. (2014)	Tripot bucket (ABAQUS^{3D})	(1) The vertical and horizontal bearing capacity factors of the tripod bucket foundation increased with increasing (*S*/*D*) and (*L*/*D*) ratios. (*S*=the spacing between each bucket and the wind turbine tower at the center, *L*=skirt length, *D*=bucket diameter) (2) The vertical (or horizontal, moment) bearing capacity of the tripod bucket foundation can be evaluated using the efficiency factor and the vertical (or horizontal, moment) bearing capacity factor of the single bucket foundation.
Liu M. M. et al. (2014)	Wide-shallow bucket (ABAQUS^{3D})	(1) The yield surface was not affected by the aspect ratio (*L*/*D*). (*L*=skirt length, *D*=bucket diameter). The vertical loading had an amplification effect on the horizontal and moment bearing capacities. (2) The horizontal loading which was in the opposite direction to the moment increased the moment capacity by 20~40%.
Zou et al. (2018)	Circular skirted bucket (ABAQUS^{3D})	(1) The effect of the surface sand layer on the response of foundations under operational loadings in sand-over-clay was profound for the ratio (*Ts*/*D*)>0.2 (*Ts*=thickness of surface sand layer, *D*=foundation diameter) (2) The failure envelopes as a function of the (*Ts*/*D*) ratio, skirt length ratio (*d*/*D*) and vertical load mobilization level ($v=V/V_{ult}$) were proposed.
Tangi et al. (2011)	Jacket (ABAQUS^{3D})	(1) The horizontal and moment bearing capacities of tri-piles foundation are increased significantly with the increasing pile diameter. (2) The bearing capacity envelope expands with the increasing pile spacing.
Yuan et al. (2012)	Jacket (ABAQUS^{3D})	(1) The stress concentration zone in front of the pile expands downward to a depth with the increase of lateral loading. (2) The horizontal bearing characteristics of pile subjected to lateral loading are influenced by the horizontal earth coefficient (K_h).
Akdag C. T. (2016)	Jacket (PLAXIS^{3D})	(1) The response of the closely spaced double piles system at the edges of the jacket foundation is superior to that of a conventional system with single piles at the edges. (1) The double piles system with a pile embedment length (*L*/2) and a pile spacing of *S*=5*D* and 6*D* provides better response. (*L*=embedded pile length of conventional system, *D*=pile diameter)

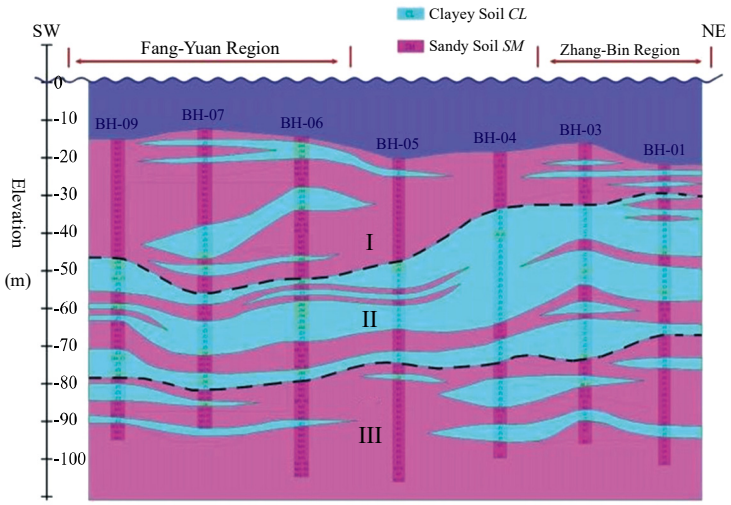

Fig. 1. The geologic profile of seafloor near the offshore water of Changhua Coast (Taiwan Power Company, 2009).

tubular steel piles with large diameter and the most widely used foundation system for supporting OWT in the offshore energy industry. The load-deformation behavior and the horizontal bearing capacity of large diameter monopiles for OWT in various marine soil strata have been investigated using 3-D finite element method (FEM) (Abdel-Rahman and Achmus, 2005; Aliasger and Gopal, 2012; Murphy et al., 2018). In addition, Zou et al. (2018) indicated that circular buckets (suction buckets or bucket foundations) are recently recognized as a potential foundation concept for supporting OWT through a jacket structure. Meanwhile, the bearing capacity, normalized failure loci (failure envelopes), failure mechanism and resulting combined capacity of suction buckets subjected to combinations of vertical, horizontal and moment loading (or *V-H-M* loading) can be determined by 3-D FEM (Zhan & Liu, 2010; Britta Bienen et al., 2012; Zou et al., 2018). The ultimate load capacity, initial stiffness, overturning stability and efficiency factors (group effect) for various bucket-soil foundation systems encompassed wide-shallow bucket foundations and tripod bucket foundations have been comprehensively investigated by 3-D FEM (Achmus et al., 2013; Liu M. M. et al., 2014; Kim et al., 2014) and most of them depend on the bucket dimensions, bucket spacing, embedment depth and loading conditions. Although the mechanical behaviors of bucket foundations and monopiles have been extensively investigated, however, they are seldom used for offshore installations in Taiwan compared with jacket foundations. As concerns the effects of combined loading on the bearing capacity behavior, no investigation was performed for jacket foundations on the marine soil strata of OWF at Changhua coast of Western Taiwan. This paper reports the numerical results from a systematic numerical investigation and explores the bearing load capacity of jacket foundations on the alternative of silty sand (*SM*) and low plasticity clay (*CL*) layers subjected to the combined *V-H-M* loading. Table 1 demonstrates the comparison on investigating various potential foundations concept for supporting OWT using 3-D FEM.

In this study, the lateral loading test of the model pile for support structure of OWT (Zhu et al., 2010) was firstly selected for 3-D numerical simulation. The suitability of the numerical procedures and material model parameters were verified by inspecting the coincidence between simulation results and testing measurements. Due to lack of loading information in Taiwan, the combined loadings adopted for numerical analyses were referred to several engineering case histories (Byrne and Houlsby, 2003; Liu B. X., 2009; Duan et al., 2010; Rong et al., 2010; Zhang et al., 2010; Stavros et al., 2011; Chen et al., 2012; Kourkoulis et al., 2012; Yan et al., 2013; Liu R. et al., 2014). In addition, the geological layered profile and soil material model parameters required for analyses were determined using the detailed geological drilling data (19 offshore boring logs) from the seabed of OWF nearby Changhua coast. Further, a series of parametric studies were performed on the pile diameter (*D*), pile length (*L*) and pile spacing (*S*) of jacket foundation using 3-D FEM and the ultimate bearing capacity envelopes (or failure envelopes) under *V-H-M* combined loading were set up simultaneously using numerical results. Eventually, the failure envelopes can be applied as references in the preliminary design of pile foundation for jacket support structure of OWT in Taiwan.

II. ANALYSES OF MARINE SOIL STRATA IN THE OFFSHORE WIND FARM OF CHANGHUA COAST

de Vries and van der Tempel (2007) suggested that the in-situ environmental data of OWF required for the design, analysis and construction of jacket foundations should comprise wave, current, meteorological, marine soil strata, and earthquake information. As a result, the marine soil layers and their associated soil material model parameters in the OWF of Changhua coastal area of Western Taiwan were determined

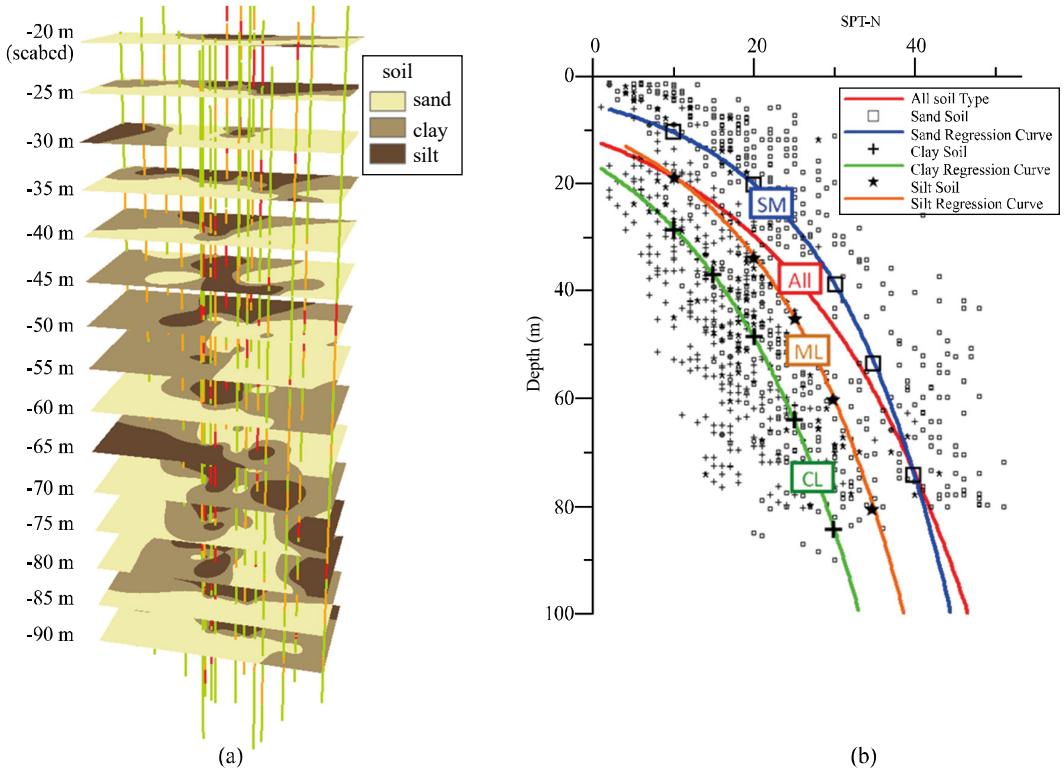

Fig. 2. Subsurface information of OWF at Changhua coast (a) Spatial distribution of marine soil strata within -20 ~ -90 m of depth (b) Regression curves of *SPT* values varied with depth.

based on the 19 geological drilling boreholes and boring logs from the research reports (Executive Yuan, Atomic Energy Council, 2014). Thickness of soil layers, soil classification and *SPT-N* value, the geological profile in the OWF of Changhua coast can be drawn as Fig. 1 (Taiwan Power Company, 2009) and the depth profile of the seabed shows that soil layers are alternate layers of sandy soil and clayey soil. Conclusively, the typical soil strata of OWF consist of silty sand layer (*SM*), low plasticity clay layer (*CL*) and silt layer (*ML*). Based on the 19 geological boring logs, the soil types for different depths were estimated using the spatial interpolation method (Kryking Differential Method, KDM) and the soil spatial distribution from elevation -20 m (at seabed surface) down to elevation -90 m was illustrated by GIS with depth spacing of 5 m as shown in Fig. (2a). Seawater of Changhua coast has an average depth of 20 m and the sea surface is selected as the datum of elevation. Eventually, the interpolation results were used as a reference of soil strata for setting up the 3-D numerical model. In addition, using the *SPT-N* data from the 19 boreholes, the regression curves of the *SPT-N* value and depth for *SM*, *ML*, *CL* and entire soil stratum were drawn as Fig. (2b). The regression models were adopted as references to inspect the *SPT-N* value of soil strata at various depths (z) and finally used to evaluate the relevant material model parameters for numerical analysis.

III. FOUNDATION TYPE FOR JACKET SUPPORT STRUCTURE OF OFFSHORE WIND TURBINE AND COMBINED LOADING

1. Group Pile Foundation for Jacket Support Structure (Jacket Foundation) of Offshore Wind Turbine

Offshore wind turbines must be fixed on the seabed through the support structure and foundation (Hammar et al., 2010). In addition to withstanding self-weight of structure, wind load, wave, tidal, seismic and other external forces, the foundation of OWT must also meet the requirements of rigidity, inclination and vibration frequency from OWT itself. To adapt to the conditions of different water depths and marine soil strata, the foundation of OWT has different types in practice. In this study, the offshore wind farms are distant from the Changhua coast about 2~6 km with water depth of 15~26 m. Considering the suitability of various support structures and foundation types of OWT in foreign countries and the field conditions in the OWF of Changhua coast, jacket support structures with three or four tubular steel pile foundations (jacket foundations) are used for supporting the OWT in deep water condition in Taiwan, as illustrated in Fig. 3. A jacket support structure is a welded tubular space frame structure with three or four legs. The bracing system between the legs provides the stiffness to the structure and acts as a buckling resistor inside the legs. The loadings are transferred to the seabed by axial forces in the

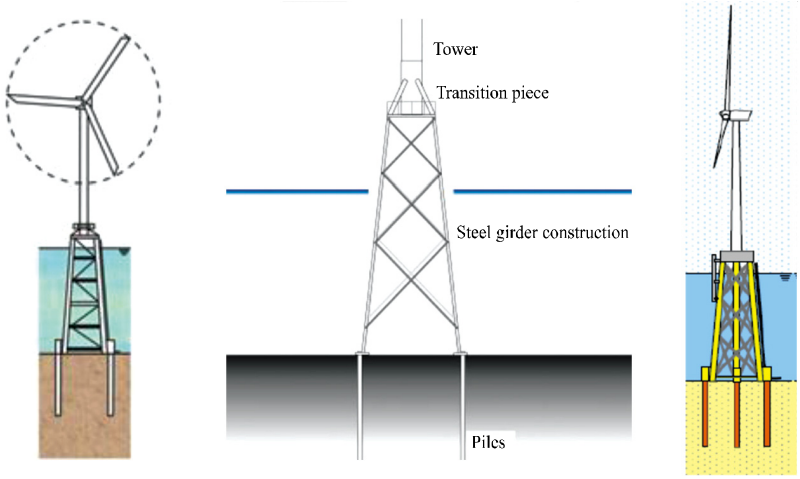

Fig. 3. Jack support structure and group pile foundation (jacket foundation) for offshore wind turbine (a) Alpha Ventus Wind Farm (2005~2010) (b) Hammar et al. (2010) (c) W. de Vries (2007).

members. W. de Vries (2007) indicated that the main advantages of the jacket structure for the application in offshore wind foundations are the jacket offers a large resistance to overturning moments. Meanwhile, jacket structure is a light and efficient construction and saves material compared to the monopile in deep water condition. Currently, the most widely used support structure is the four-leg jacket and therefore only the four-leg jacket was studied in this article.

Tangi et al. (2011) studied the bearing capacity behaviors of tri-piles foundation for jacket supporting structure (or jacket foundations) of OWT by changing diameter and spacing of piles via 3-D FEM. Akdag (2016) found that, at the edges of the jacket foundations, the contribution and overall foundation response of closely spaced double piles is superior to those of conventional single pile. Although the jacket foundation design for OWT has been reviewed and studied by several researchers (Byrne and Houlsby, 2003; Duan et al., 2010; Zhang et al., 2010; Tangi et al., 2011; Yuan et al., 2012; Akdag, 2016), however, in Taiwan, the responses of the foundation have not yet been evaluated considering the geotechnical characteristics in the OWF of Changhua coast. The combined loading applied to individual piles of jacket foundations increases considerably with the increase of the water depth and the jacket foundation is appropriate for water depth up to 30~80 m (Achmus et al., 2007; Shi et al., 2013). In such circumstances, the jacket foundation of wind turbines in the OWF of Changhua coast with the water depth of 15~26 m may guarantee a satisfactory bearing capacity against loadings. Therefore, this study concentrates on the mechanical behaviors of foundation with four piles positioned at the edge corners of jacket support structure.

2. Consideration of Combined Loading

In the operation period, the jacket foundations are required to resist the combined *V-H-M* (*V*ertical-*H*orizontal-*M*oment) loading imposed by dead loads (weights of wind turbine structure, permanent facilities, and auxiliary structures), live loads (erection or removal of facilities, consumption or supplement of objects and liquid matters, ship berthing or lifting transport) and environmental loads (wind, wave, current, earthquake) according to the RP 2A-WSD standard of American Petroleum Institute (API, 2000). The RP 2A-WSD standard provides a detailed explanation and suggestion on wind load calculations. In addition, several equations for wave and current load calculations are also demonstrated in 61400-1 international standard of International Electrotechnical Commission (IEC, 2005). The design loads adopted for the analysis and design of OWT foundations were mostly estimated according to the measurement and instrumentation in the OWF or the previous design experiences in China (Liu, 2009; Duan et al., 2010; Zhang et al., 2010; Yan et al., 2013; Liu et al., 2014). Stavros et al. (2011) adopted the wave height of 16 m and wind speed of 60 m/sec of 50 years return period to determine the ultimate wave force and wind load. Liu (2009) used the design load resulted from the external loadings including self-weight, wind load, wave force, and tidal force to perform the numerical analyses on the pile foundation of OWT with device capacity of 3.0 MW, reel diameter of 90 m and wheel hub height of 80 m.

Due to the complexity and uncertainty of marine environment and frequent earthquakes and typhoons in Taiwan, extreme environmental conditions and the seismic load must be taken into account for the design loads. As Taiwan still lacks the construction case histories of OWT and on-site monitoring data, this study integrates the design loads (M_x, M_y, M_z, F_x, F_y, F_z) from the above references and uses the horizontal load F_x=6.00 MN (=H), vertical load F_z=12.00 (=V) and moment load M_x= 250.00 MN-m (=M) as the input values of a design example in the last section.

The OWT unit adopted in Taiwan is similar to NREL-5 MW (baseline offshore wind turbine) and Jonkman et al. (2009) has a detailed description of the specifications of this model.

Table 2. Material model parameters of (a) soil (b) tubular steel model pile for lateral loading test in laboratory.

(a)

Soil Layer	γsat (kN/m3)	ν′	c′ (kPa)	ϕ′ (°)	ψ (°)	E′ (kPa)
Saturated Silty Sand (SM)	17.5	0.3	0.2	28.5	0	1000

(b)

Diameter D (m)	Thickness t (m)	Length L (m)	γ (kN/m^3)	Es′ (×10^8 kPa)	Fmax (kN)	Tmax (kN/m)	A (×10^{-4} m^2)	I_2 and I_3 (×10^{-6} m^4)
0.114	0.0025	2.6+4.4	76.94	2.30	0.95	4.66	8.757	1.362

Meyerhof (1976):

(1) Fmax=$A_p \times q' \times N_q$ (for sand), $F_{max}=A_p \times c_u \times N_c$ (for saturated clay), in which, A_p=area of pile tip, q'=effective vertical stress at the level of the pile tip, N_q & N_c=the bearing capacity factors, c_u=undrained shear strength (cohesion) of the soil supporting the pile tip.

(2) Tmax=$\sum p \times f = \sum p \times (K_o \times \sigma_v' \times \tan\delta)$, in which, p=perimeter of the pile section, f=unit friction resistance at any depth, K_o=(1-sinϕ′)=at-rest pressure coefficient, ϕ′=effective friction angle of soil, σ_v'=effective vertical stress at any depth, δ =soil/pile interface friction angle =(0.5~0.8)×ϕ′

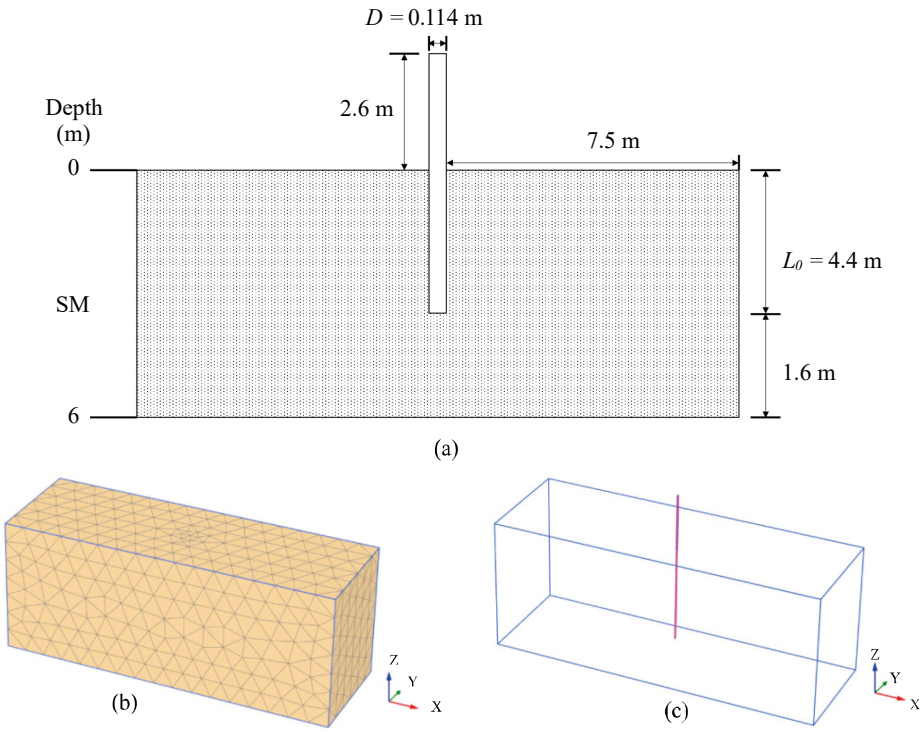

Fig. 4. Three-Dimensional numerical model of lateral loading test of tubular steel model pile (a) geometric configuration of soil trough and tubular steel model pile (b) finite element mesh (c) structure elements for model pile.

Accordingly, this study performs a systematic numerical analysis to investigate the bearing capacity of four-pile foundation with square configuration for jacket support structure (jacket foundation) of OWT with device capacity of 5.0 MW.

IV. LATERAL LOADING TEST OF LARGE SCALE MODEL PILE FOUNDATION FOR OFFSHORE WIND TURBINE AND NUMERICAL VERIFICATION

The monitoring and instrumentation data based on the full scale multi-pile jacket foundation for OWT are rare in the literature. Accordingly, prior to the parametric study, the validity of the numerical procedures and material models was verified with the large scale lateral loading test of model pile conducted by Zhu et al. (2010) in laboratory. As shown in Fig. 4(a), the silty sand (*SM*) layer was compacted by layers with a 30 cm lift in a soil trough with dimensions of 15 m×5 m×6 m (=length×width×height). The basic engineering properties of silty sand (*SM*) include specific gravity G_s=2.69,

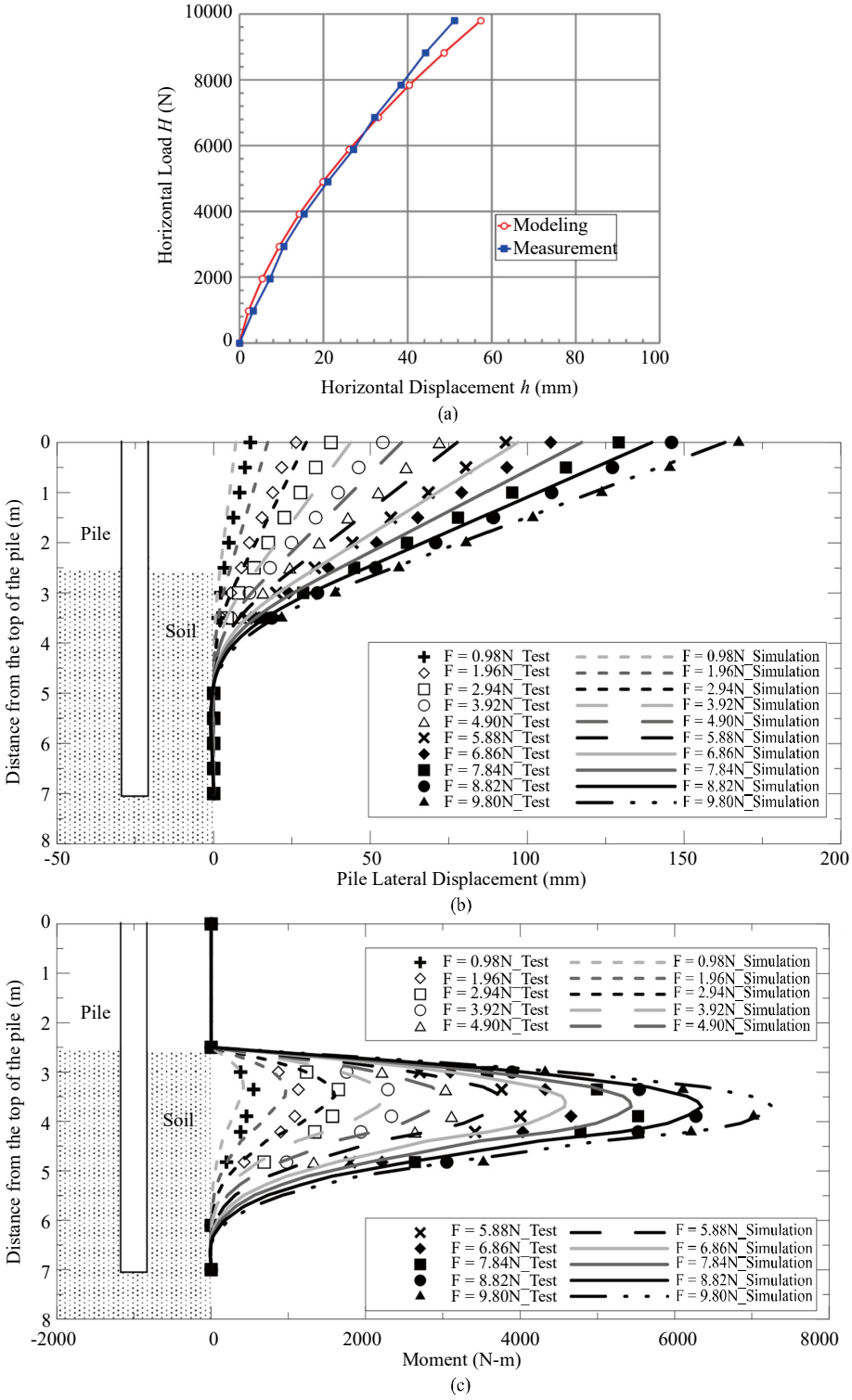

Fig. 5. Comparisons between simulation and measurement (Zhu et al., 2010) of lateral loading test of steel pipe model pile (a) lateral loading versus lateral displacement curve of the pile shaft above the trough of 0.1 m height (b) distribution of lateral displacement along the pile shaft for different loading stage (c) distribution of bending moment along pile shaft for different loading stage.

plastic limit PL=22.6, liquid limit LL=31.7, water content w=32.5 %, saturated unit weight γ_{sat}=17.5 kN/m^3, and average permeability K_{ave}=4.2×10^{-6}~6.4×10^{-6} m/sec. The compacted silty sand was modeled as an elastic-perfectly plastic material obeying Mohr-Coulomb yield criterion with non-associated flow rule (M-C soil model).

Table 3. Mohr-Coulomb material model parameters of marine soil strata.

Soil Layer	Depth (m) Thickness-t (m)	SPT-N value	γ_{sat} (kN/m^3)	c′ (kPa)	ϕ′ (°)	ψ (°)	E′ (×10^3 kPa)	ν′
SM1	0.00~4.20 t=4.20	6	18.28	20	25	0.0	4.60	0.30
SM2	4.2~14.77 t=10.57	11	18.91	20	28	0.0	8.43	0.30
SM3	14.77~39.30 t=24.53	24	19.10	20	33	3.5	18.38	0.32
CL1	39.30~49.60 t=10.30	19	18.92	13	30	0.0	15.54	0.30
SM4	49.60-60.03 t=10.43	38	19.35	20	35	5.0	29.11	0.32
CL2	60.03~62.46 t=2.43	20	18.74	13	30	0.0	16.31	0.30
SM5	62.46~71.23 t=8.77	39	19.11	20	35	5.0	29.87	0.32
CL3	71.23~74.40 t=3.17	24	19.01	13	30	0.0	19.39	0.30
SM6	74.40~80.00 t=5.60	40	19.37	20	35	5.0	30.64	0.32

A tubular steel model pile with closed end and dimensions of 114 mm×7000 mm×2.5 mm (=exterior diameter×length×thickness) was installed at the middle of soil trough and subjected to a horizontal loading. The model pile head was extended above the soil surface for 2.6 m and the horizontal loading was applied to the model pile at a point 0.1 m above the soil surface. The model pile segment above and below the soil surface were simulated by beam element and embedded pile element respectively. The number of nodal point, integration point and the interpolation function of these two types of structural elements are identical. Accordingly, the structural integrity can be maintained in the numerical model constantly. The main difference of these two types of structural elements is that the embedded pile element needs to interact with the surrounding soil strata thru the maximum end resistance of the pile tip (=F_{max}) and maximum frictional resistance along the pile shaft (=T_{max}) (Meyerhof, 1976). The 3-D numerical model of geometric configuration and finite element mesh are exhibited in Figs. 4(b) and (c). The material model parameters of compacted silty sand and tubular steel model pile are coincident with those determined in the laboratory and presented in Table 2.

The numerical model was validated by comparing the load/displacement curve (or *H*~*h* curve) at the load applied point (0.1 m above soil surface), the pile lateral displacement, and the pile bending moment of modeling with those of measurement. The *H*~*h* curve at load applied point obtained by 3-D numerical modeling exhibits an excellent coincidence with the experiment curve, as shown in Fig. 5(a). The slight deviation of the simulation from the measurement may be resulted from the incapability of the constitutive model to capture the entire soil/structure interaction behaviors and the properties of soil specimen preparation in the large scale test. In addition, as shown in Fig. 5(b) and (c), the distributions of the pile lateral displacement and the pile bending moment for each loading step of modeling are all in a good agreement with those of measurement. For both the modeling and measurement, the fixed point with zero lateral displacement of model pile situates 2.0 m below the soil surface (or 4.6 m=2.6 m+2.0 m below the pile head, see Fig. 5(b)) and the maximum bending moment occurs within 1.0~1.5 m below the soil surface (or below the pile head of 3.6~4.1 m, see Fig. 5 (c)). Conclusively, the suitability of numerical procedures and input material parameters of *M*-*C* soil model for the 3-D numerical modeling of lateral loading test of model pile are verified.

V. NUMERICAL ANALYSIS AND PARAMETRIC STUDY OF BEARING CAPACITY OF GROUP PILE FOUNDATION FOR OFFSHORE WIND TURBINE

1. Design Parameters

According to API (2000), the design standard of pile foundation for OWT, the thickness of tubular steel piles (*t*) can be given by *t* (mm)≥ 6.35+(*D*/100) and *D* (mm) is the pile diameter. In this study, a thickness *t*=50 mm was used for numerical analyses. For the configuration of group pile, in principle, the pile spacing (*S*) is not less than 2.5 times pile diameter (*S* ≥ 2.5*D*). In addition, due to the lack of experience in the development of OWF in Taiwan, the design parameters of the tubular steel pile are determined by referencing to the

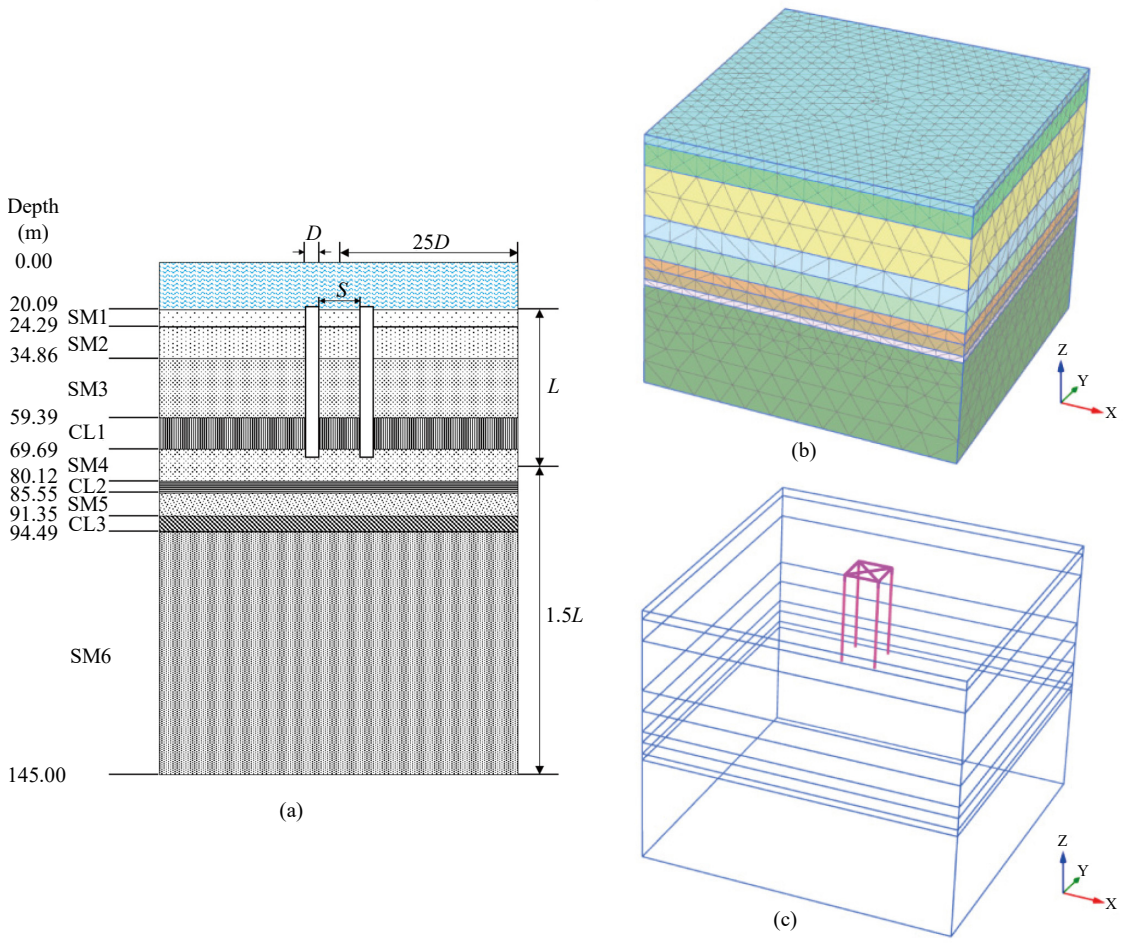

Fig. 6. Three-Dimensional numerical model for ultimate bearing capacity analyses of single and group pile foundation (a) soil strata, configuration of pile, and geometry boundary (b) finite element mesh(c) structural model of group pile.

foreign design case histories. A parametric study was carried out to identify the effects of pile length L=30, 40, 50 m (=15×D, 20×D, 25×D; D=2 m), pile diameter D=1.0, 1.5, 2.0, 2.5, 3.0 m and pile spacing S=12, 16, 20 m (=6×D, 8×D, 10×D; D=2 m) on the behaviors of a jacket foundation supported by multi piles in a typical marine clayey/sandy soil strata in the OWF of Changhua coastal area at Western Taiwan. The ultimate bearing capacities of the vertical, horizontal, moment, and combined loadings for single and group pile are determined in this study.

2. 3-D Numerical Model

As shown in Fig. 6, a 3-D numerical model was developed according to a four-pile (2×2 tubular steel pile) supported jacket foundation for OWT (5 MW) and the offshore marine soil strata and utilized for a parametric study. As displayed in Figs. 6(a) and (b), a preliminary trial computation was performed to determine the model dimension of 50×D (D=pile diameter) for length and width whereas of 2.5×L (L=pile length) for depth. The average water depth of 20.09 m (Depth 0.00~20.09 m in Fig. 6(a)) above seabed was adopted in the numerical modeling. Eventually, the numerical model can achieve an efficient and accurate calculation and eliminate the boundary effects on numerical solutions. In addition, the pile head is extended 1.0 m above the seabed and the four piles in the pile group are connected at the pile head by a pair of cross steel tied bar, as shown in Fig. 6(c). Initial effective stresses and pore pressure of soil strata are calculated by K_o-condition and phreatic line-condition respectively.

3. Material Model Parameters

Through the data analyses of the 19 geological drilling boreholes mentioned earlier, although the profile of marine soil strata at Changhua coastal area varies greatly but there is only a small difference in soil strength parameters. The marine soil strata were simulated by volumetric soil element with Mohr-Coulomb (*M-C*) material constitutive model and the required material model parameters are summarized in Table 3 including elastic modulus E', cohesion c', friction angle ϕ', dilation angle ψ, and Poisson's ratio ν'. The *M-C* material model parameters for marine soil strata were determined according to the *SPT-N* value and various laboratory strength

Table 4. Material model parameters of tubular steel pile.

Pile diameter D (m)	Thickness of tubular steel pile t (m)	Pile length L (m)	Unit weight γ_{steel} (kN/m^3)	Elastic modulus E'_{steel} ($\times 10^8$ kPa)	End resistance F_{max} (kN)	Frictional resistance T_{max} (kN/m)	Cross sectional area A (m^2)	Moment inertia I_2 & I_3 (m^4)
2.0	0.05	40	76.94	2.30	85.65	301.4	0.3063	0.1457

Referring to Table 2, (F_{max}) and (T_{max}) are determined using Meyerhof's (1976) method.

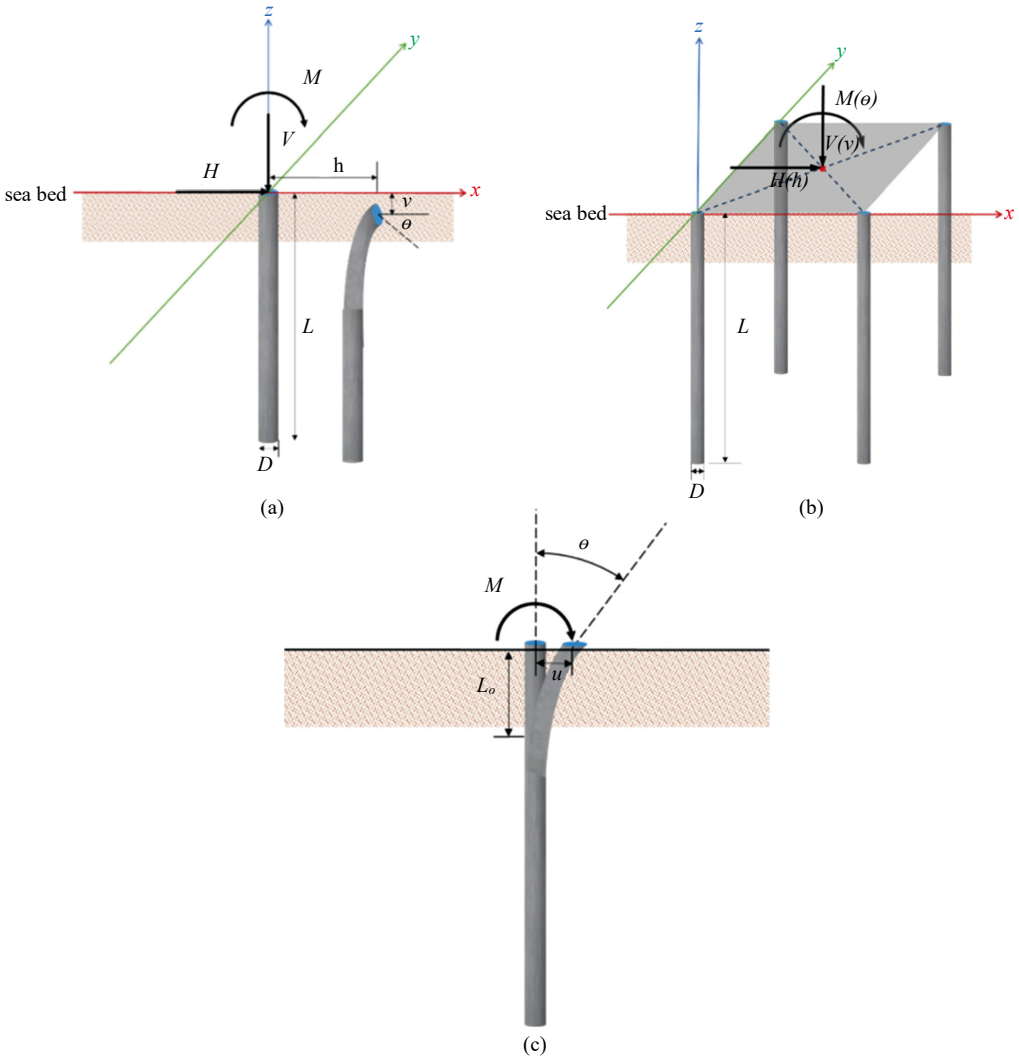

Fig. 7. Combined loading for the numerical analyses of bearing capacity (a) single pile (b) group pile (c) rotational angle θ under bending moment.

tests of undisturbed samples. The initial effective overburden stresses of soil strata were modeled using K_o-condition where K_o=(1-sinϕ') (Jacky, 1944).

The tubular steel piles were modeled using beam element from seabed to pile head (Elevation=-20.09 m~-19.09 m) and using embedded pile element beneath the seabed (Elevation=-20.09 m~-60.09 m, for pile length L=40 m). The cross steel tied bar used to connect the piles at the pile head in the pile group is simulated by beam element. The embedded pile element is different from the beam element and it needs two extra inputs, namely, a maximum end resistance (F_{max}) at pile tip and a maximum frictional resistance (T_{max}) along pile shaft which are used to determine the bearing capacity. The tubular steel piles in the pile group were simulated by the linear elastic material model and the material model parameters required for the numerical simulation are listed in Table 4.

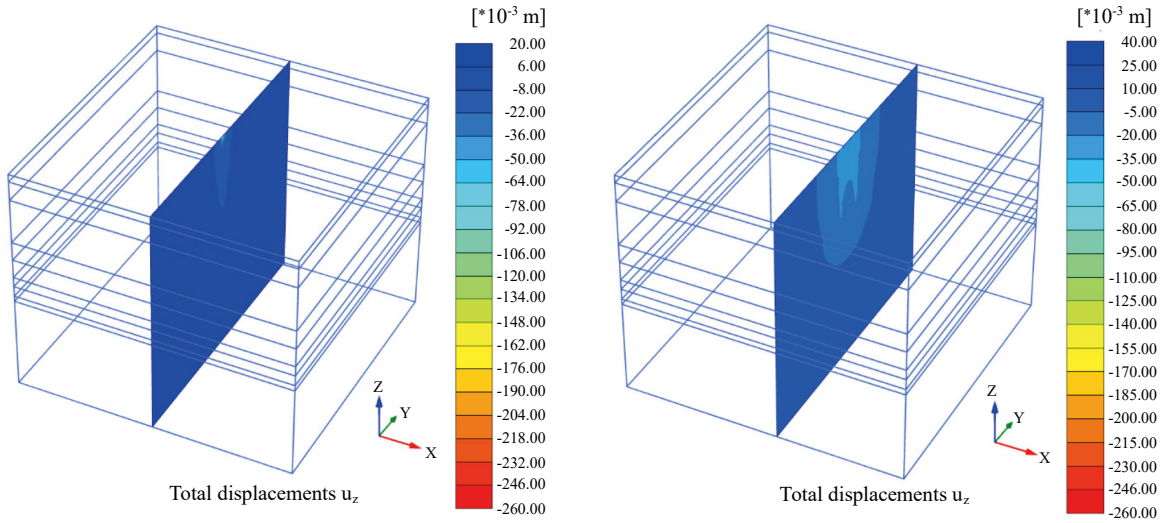

(a) v=-0.10 m for $(V_{ult})_{single}$=6.708 MN

(b) v=-0.18 m for $(V_{ult})_{group}$=22.233 MN

Fig. 8. Vertical displacement contour under ultimate condition subjected to vertical displacement loading along (a) longitudinal profile at x=0 m for single pile (b) longitudinal profile at x=8 m for group pile.

4. Criterion for the Determination of Ultimate Bearing Capacity (or Ultimate Load Capacity)

For the displacement criterion to determine the ultimate bearing capacity of pile foundation, Vesic (1973) proposed the vertical load of pile is equivalent to its ultimate load capacity if the settlement of pile head approaches 10 % of the pile diameter. In addition, according to the Building Infrastructure Design Specifications (Ministry of the interior, Taiwan, 2001), in principle, the horizontal displacement of pile foundation (h) should be limited within the allowable value ($h_{allowable}$) which mostly approximates 1 % of pile diameter D ($h \leq h_{allowable}$=0.01×D). For the failure criterion of soil material, the ultimate load can be defined as the corresponding load to cause the onset of plastic yielding of the soil stratum adjacent to the piles. In this study, the ultimate load capacities of pile foundation subjected to the combined loading is defined as the applied loads immediately leads to a plastic yielding of soil stratum (or the first occurrence of any plastic point observed in the numerical model). Namely, the capacities were obtained with displacement-controlled loads applied to the pile head of single pile or the center of pile group until failure of soil mass surrounding the pile was reached and demonstrated through the occurrence of plastic points with increasing displacement.

5. Application of Combined Loading

The reference point for applying displacement loads is located at the pile head of single pile and the center of pile group as shown in Fig. 7(a)~(c). The ultimate vertical (V_{ult}), horizontal (H_{ult}) and moment (M_{ult}) capacities were calculated with displacement-controlled loads of vertical (v), horizontal (h) and rotation (θ) displacements respectively. (e.g. V_{ult} was obtained for the displacement load v only and in the absence of displacement loads h and θ). General combined V-H-M loading was achieved by firstly applying a fixed moment loads (M) and subsequently a vertical displacement and horizontal displacement increments (δv) and (δh) were imposed on the reference point with fixed displacement increment ratio (δv/δh) equals to 0.5, 1 and 2 proposed by Supachawarote et al. (2004).

Referring to the previous researches, the maximum applied vertical or horizontal displacement load (v_{max} or h_{max}) approximates 0.30 m and the maximum applied moment load (M_{max}) is about 200 MN-m. Meanwhile, the plastic yielding or plastic failure of soil mass mostly occurs under a displacement load smaller than 0.30 m or a moment load lower than 200 MN-m (Zhan and Liu, 2010; Haiderali and Madabhushi, 2012; Liu M. M. et al., 2014; Akdag, 2016, Murphy et al., 2018). After a large quantity of trial calculation, it can be found that the marine soil in the OWF of Changhua coast can constantly reach plastic yielding under a displacement load of 0.1 m or a moment load of 100 MN-m. Eventually, in this study the plastic yielding criterion of soil mass under various combined loadings was adopted to construct the failure envelopes of ultimate bearing capacity of jacket foundation for OWT in the OWF of Changhua coast at Western Taiwan.

VI. RESULTS AND DISCUSSIONS

The modeling results of bearing capacity and deformation behavior of multi-pile foundation for jacket support structure (jacket foundation) are interpreted and discussed in this section. In this study, the ultimate load capacities of pile foundation in response to various combined loadings, V, H, M, V-H and V-H-M loadings are determined as the applied loads immediately leads to a plastic yielding of soil strata. Meanwhile, the onset of plastic yielding is corresponding to the first

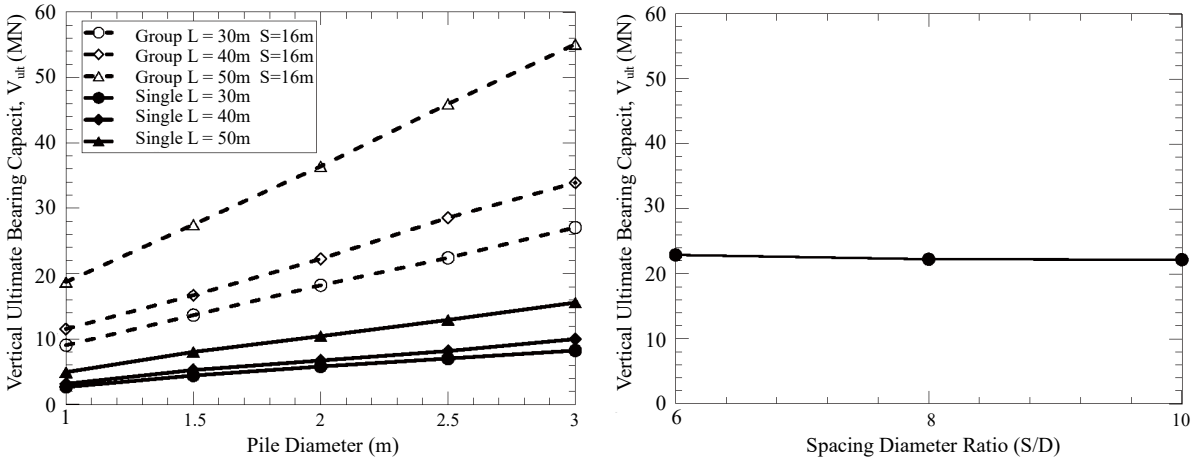

Fig. 9. (a) Vertical bearing capacity (V_{ult}) of single and group pile (spacing S=16 m) for different pile lengths and diameters (b) effect of the spacing of group pile (D=2.0 m, L=40) on vertical bearing capacity $(V_{ult})_{group}$.

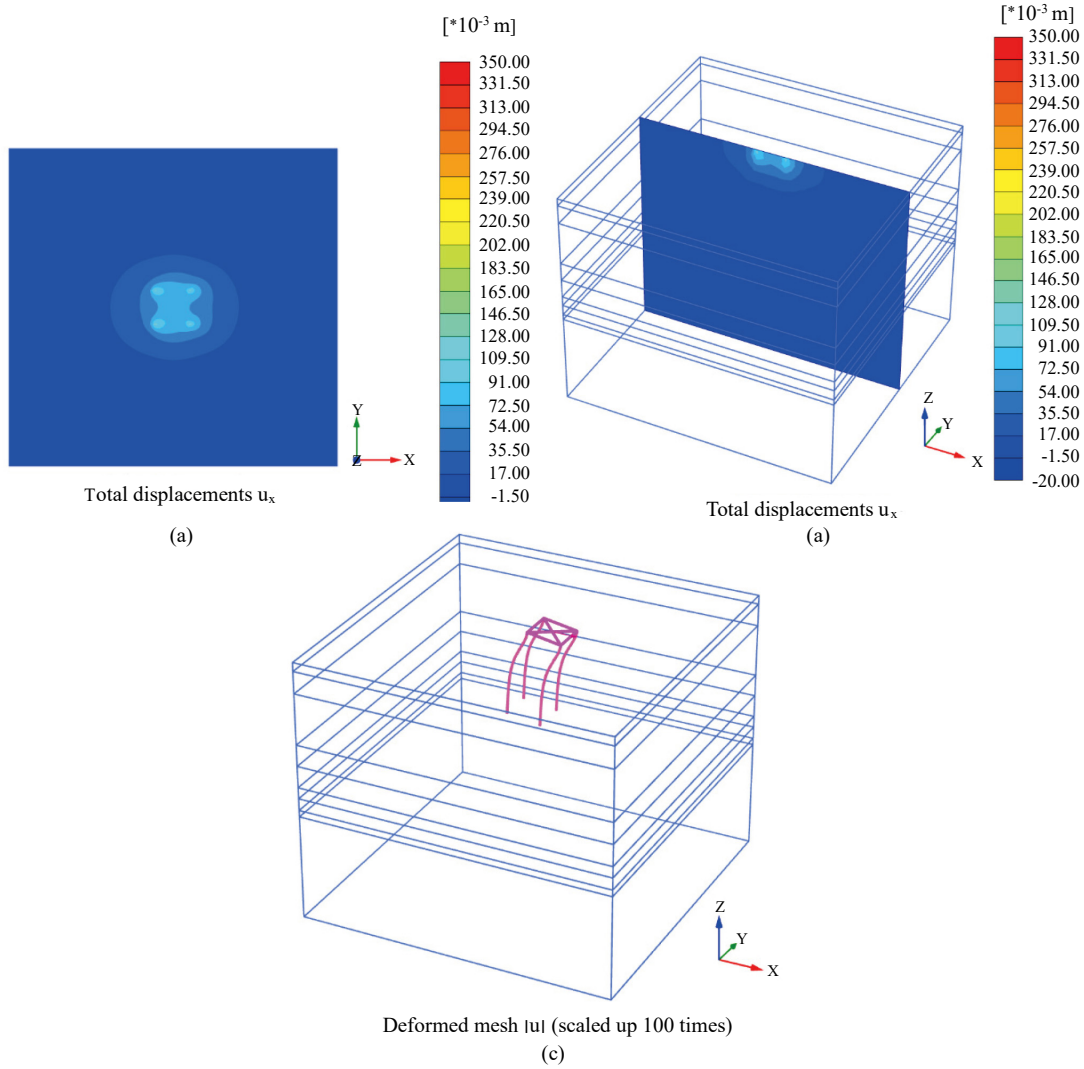

Fig. 10. Horizontal displacement contour under ultimate condition subjected to horizontal displacement loading (a) transverse profile at the seabed elevation (b) central longitudinal profile at y=8 m (c) displacement mode of group pile for a horizontal displacement load h=0.10 m.

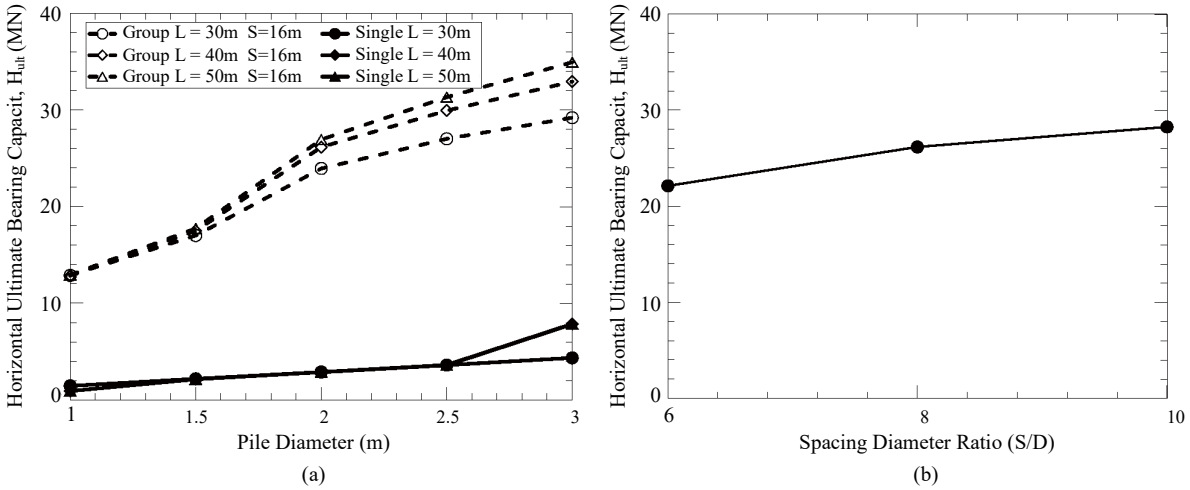

Fig. 11. Horizontal bearing capacity of single and group pile for (a) different pile diameters *D* and pile lengths *L* (b) different spacing *S* (=6×*D*, 8×*D*, 10×*D*; *D*=2.0 m, *L*=40 m).

occurrence of any plastic point in the numerical model. In the end, the normalized *V-H* and *V-H-M* failure envelopes for group pile foundations subjected to combined loadings are expressed in terms of *L*, *D*, and *S* and as functions fitted by elliptical shape curves.

1. Ultimate Vertical Bearing Capacity (or Ultimate Vertical Load Capacity) (V_{ult})

Figure 8 reveals the vertical displacement contour (u_z) of soil strata at ultimate state for a single pile (*D*=2.0 m, *L*=40 m) and group pile (*D*=2.0 m, *L*=40 m, *S*=16 m, 2×2=4 piles) subjected to the vertical displacement loading (*v*). The soil layer begins to undergo a plastic yielding when a vertical displacement loading *v*=0.18 m is applied to group pile and *v*=0.10 m to single pile. The ultimate vertical bearing capacity corresponding to the onset of the plastic yielding of soil layer is $(V_{ult})_{single}$=6.708 MN for single pile and $(V_{ult})_{group}$=22.233 MN for group pile. The plastic yielding zone is mainly concentrated in the loose silty sand layer (*SM*, *SPT-N*= 2~10) of the seabed surface near the pile head.

As shown in Fig. 9(a), it is apparent that the vertical bearing capacities of single and group pile ascends with the increase of pile length (*L*) and pile diameter (*D*). However, the influence of the pile spacing (*S*) on the vertical bearing capacity of group pile is insignificant (see Fig. 9(b)). Under various (*D*), (*L*) and (*S*) combinations, the vertical bearing ratio $(R_V)_{ult}=[(V_{ult})_{group}/(V_{ult})_{single}]$=2.92~3.79<4.0 can be obtained. This demonstrates that the stiffness of group pile is higher than that of single pile and the pile group effect of the vertical loading due to overlapping of soil stressed reaction zones is observed. Kim et al. (2014) performed a series of model pile tests with various closely spaced pile layouts and indicated that stress overlapping caused by group interaction reduces the load bearing capacity.

2. Ultimate Horizontal Bearing Capacity (or Ultimate Horizontal Load Capacity) (H_{ult})

Figure 10(a) ~ (c) show the transverse and longitudinal profiles of horizontal displacement contour (u_x) of soil strata and displacement mode of the group pile (*D*=2.0 m, *L*=40 m, *S*=16 m, 2×2=4 piles) subjected to horizontal displacement load (*h*)=0.10 m with the horizontal ultimate bearing capacity $(H_{ult})_{group}$=26.159 MN. At the meantime, the horizontal ultimate bearing capacity $(H_{ult})_{single}$=2.865 MN of the single pile (*D*=2.0 m, *L*=40 m) can be obtained under horizontal displacement load (*h*)=0.08 m. The plastic yielding zone is mainly concentrated in the seabed surface around the pile/soil interface of pile head and limits within a shallow depth of 4.0×*D*~6.0×*D* below the seabed surface. The soil layer in this depth range is classified to be the loose silty sand (*SM*, *SPT-N*=2~10). The horizontal displacement of soil mass surrounding the pile decreases significantly with the increasing depth and this is identical with the numerical results from Tangi el al. (2011).

According to Fig. 11(a), it is obvious that pile diameter *D*>2.5 m for single pile and *D*>1.5 m for group pile, the horizontal bearing capacity (H_{ult}) significantly enhances with the increasing pile diameter and pile length. These are identical with the numerical results of tri-piles foundation presented by Tangi et al., (2011). In addition, as shown in Fig. 11(b), the horizontal loading efficiency is influenced by the pile spacing due to stress overlapping of the soil resisting zones for the individual piles in the group. It can be found that the horizontal bearing capacity of group pile $(H_{ult})_{group}$ noticeably increases with the increasing pile spacing *S* (*S*=6×*D*→10×*D* or *S*=12 m→20 m for *D*=2.0 m) and this implies that the stress overlapping of soil resisting zone around laterally loaded piles caused by group interaction can be mitigated by extending the pile spacing of individual piles. The horizontal bearing capacity of group pile $(H_{ult})_{group}$ is greatly higher than that of

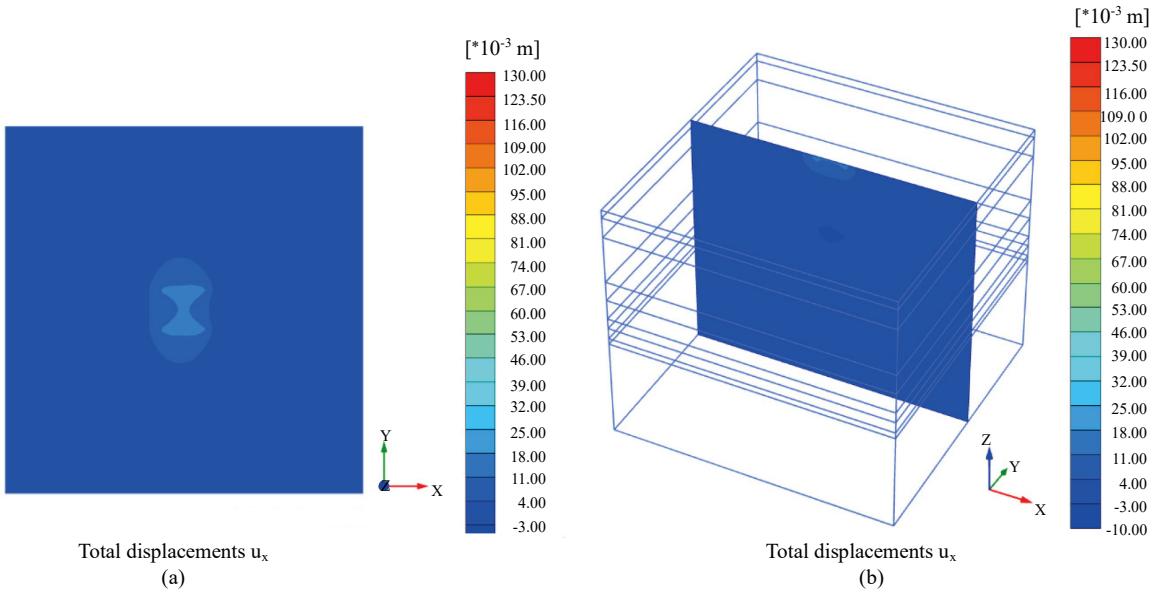

Fig. 12. Horizontal displacement contour of group pile under ultimate condition subjected to moment load (a) transverse profile at seabed elevation (b) central longitudinal profile at *y*=8 m.

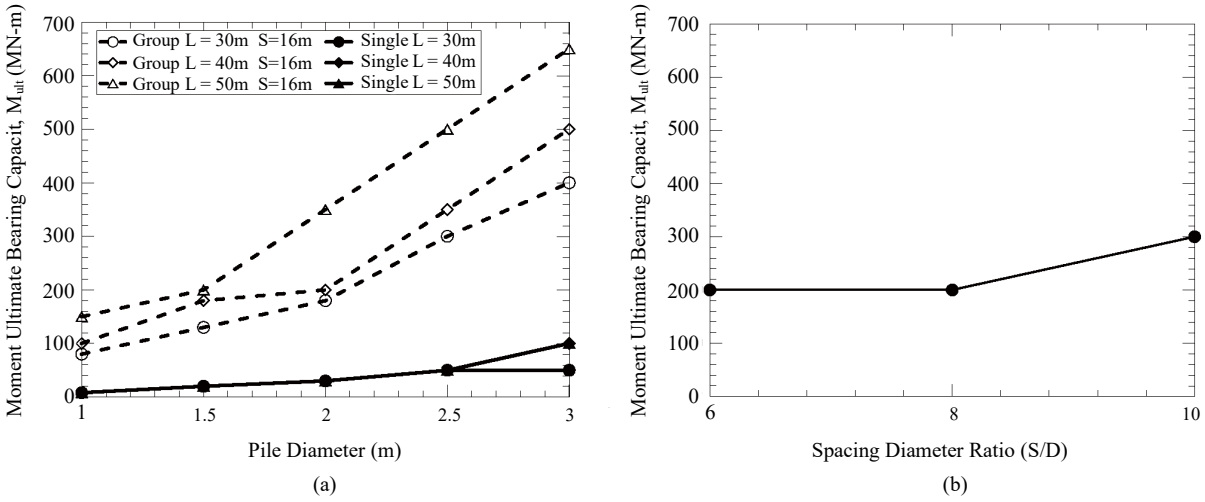

Fig. 13. Ultimate moment bearing capacity of single and group pile for (a) different pile diameters *D* and pile lengths *L* (b) different spacing *S* (=6×*D*, 8×*D*, 10×*D*; *D*=2.0 m, *L*=40 m).

single pile $(H_{ult})_{single}$ because of the comparatively higher lateral stiffness of group pile. For a specific pile spacing (S=16 m), the horizontal bearing ratio $(R_H)_{ult}=[(H_{ult})_{group}/(H_{ult})_{single}]$ is in a range of 4.2~14.3 for various combinations of (D) and (L) in numerical calculations. In summary, for a pile foundation with specific pile length (L=constant), the $(R_H)_{ult}$ value reduces with the enlargement of pile diameter and this is due to the stress overlapping of soil in between the individual piles under group interaction becomes noticeable as the pile diameter increases.

3. Moment Bearing Capacity (or Ultimate Moment Load Capacity) (M_{ult})

Figure 12 displays the transverse and longitudinal profiles of horizontal displacement contour (u_x) of soil layers with maximum horizontal displacement h_{max}=0.569 m around the group pile (D=2.0 m, L=40 m and S=16 m) when subjected to the ultimate bearing moment (M_{ult}). The corresponding pile head rotations (θ) for ultimate moment loads M_{ult}=200 MN-m (group pile) and M_{ult}=30 MN-m (single pile) are θ=0.091 and 0.354 respectively and the soil layer starts to undergo plastic yielding. Alike the case of horizontal displacement loading, the plastic yielding zone also limits within a shallow depth of 3.5×D~7.0×D below the seabed surface. Tangi el al. (2011) indicated that the effect of moment loading on the tri-pile is similar with that of horizontal loading.

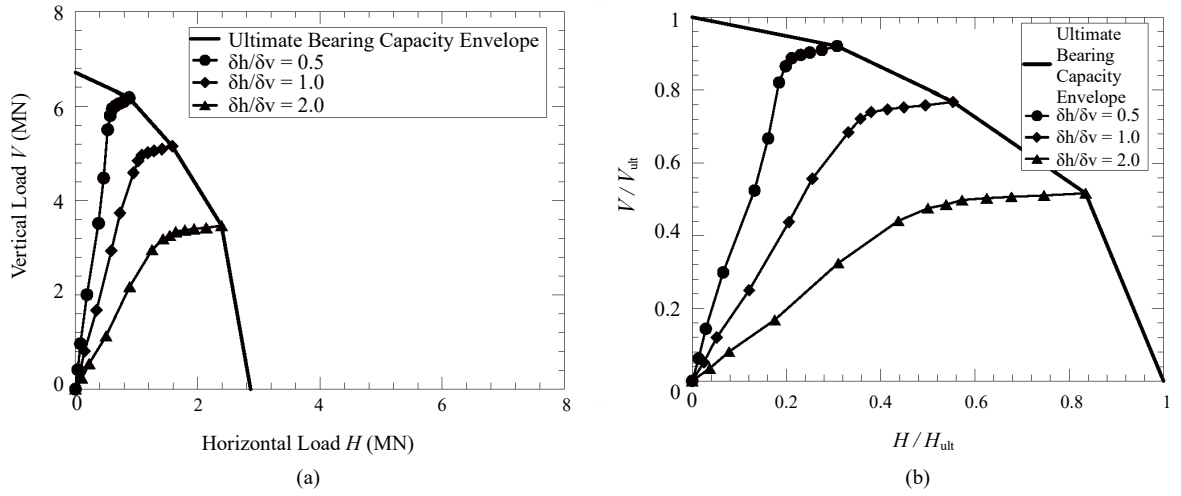

Fig. 14. ***V-H*** **loading path and** ***V-H*** **envelope of bearing capacity (*V-H* envelope) of single pile (a) dimensional (b) dimensionless with normalization (*V*$_{ult}$=6.708 MN ; *H*$_{ult}$=2.865 MN).**

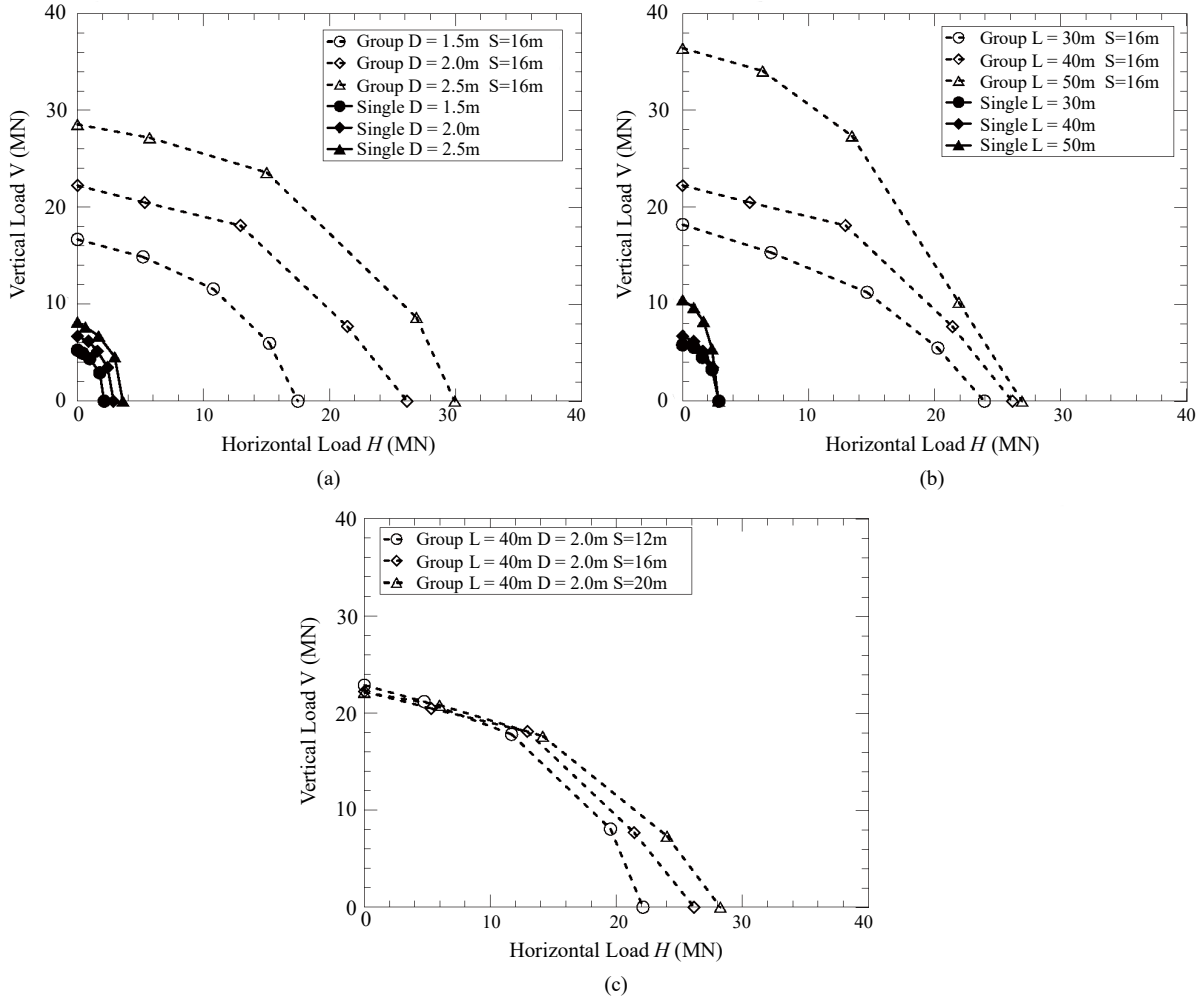

Fig. 15. ***V-H*** **envelopes of bearing capacity of single and group pile for (a) different pile diameters (*D*=1.5 m, 2.0 m, 2.5 m) (b) different pile lengths (*L*=30 m, 40 m, 50 m) (c) different pile spacing (*S*=12 m, 16 m, 20 m).**

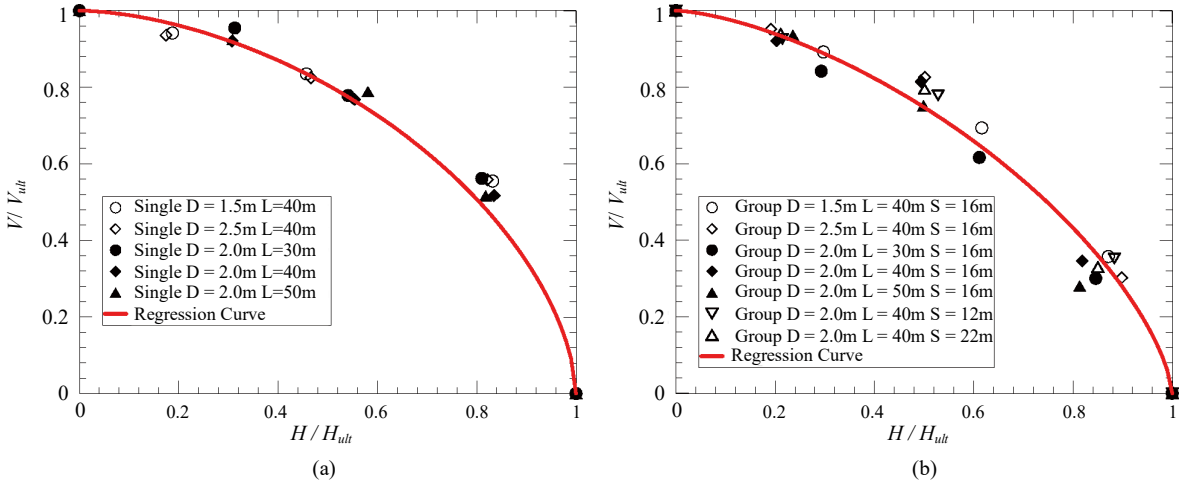

Fig. 16. Regression curve of normalized *V-H* envelope of bearing capacity without moment load (M/M_{ult} = 0) (a) single pile (b) group pile.

As presented in Fig. 13(a), the ultimate moment bearing capacity (M_{ult}) of group pile (S=16 m) apparently ascends with the extension of pile lengths (L=30→50 m) and the enlargement of pile diameters (D=1.0→3.0 m) particularly as D >1.5 m. For a specific pile spacing (S=16 m), the moment bearing ratio $(R_M)_{ult}$ (=[$(M_{ult})_{group}/(M_{ult})_{single}$]) is in a range of 4.0~18.8 for various combinations of (D) and (L) in numerical calculations. In summary, the $(R_M)_{ult}$ value decreases with the enlargement of pile diameter and increases with the extension of pile length. However, for single pile, the effects of pile lengths and pile diameters on (M_{ult}) value are obviously less than those of group pile. This situation also can be observed in horizontal bearing capacity (H_{ult}) (see Fig. 11(a)). However, the (M_{ult}) value of group pile increases with the enlargement of pile spacing S (=6×D→10×D or =12→ 20 m for D=2.0 m) only for the condition of S>16 m as shown in Fig. 13(b).

4. *V-H* Envelope of Bearing Capacity (or Ultimate *V-H* Load Capacity) (*V-H* Envelope)

As shown in Fig. 14(a), 12 loading tests for each displacement increment ratio ($\delta h/\delta v$)=0.5, 1.0 and 2 generate load paths of a single pile that start from the origin and approach the ultimate bearing capacity envelope. The ultimate bearing capacities of single pile V_{ult}=6.708 MN and H_{ult}=2.865 MN are determined according to the vertical ($\delta v\neq 0$ and δh=0) and horizontal ($\delta h\neq 0$ and δv=0) loading tests respectively. The load paths are initially following the gradients which depend on the elastic modulus of the soil surrounding the pile foundation. With the accumulation of the plastic yielding of the surrounding soil, the load paths begin to change till they reach the ultimate bearing capacity envelope which consists of 5 loading tests with ultimate bearing or load capacities. As illustrated in Fig. 14(b), the load paths gradually shift from the side of (V/V_{ult})-axis to the side of (H/H_{ult})-axis in response to the ascending of displacement increment ratio ($\delta h/\delta v$) from 0.5 to 2.0.

As displayed in Fig. 15(a) and (b), the two groups of *V-H* envelopes are similar and reflecting the trend of expansion of failure envelopes with increasing plie diameter D (=1.5 m →2.5 m) and pile length L (=30 m→50 m) for single and group pile. It is apparent that the failure envelopes in *V-H* space are a function of both D and L. Furthermore, it can be seen in Fig. 15(b) that the expansion of the envelopes with increasing pile length at the vertical load axis (V-axis) side is more evident than that at the horizontal load axis (H-axis) side. This indicates that the influence of pile length on the vertical bearing capacity (V_{ult}) is much higher than that on the horizontal bearing capacity (H_{ult}). Similarly, as shown in Fig. 15(c), the expansion of the envelope with increasing pile spacing S merely occurs at the H-axis side and not at the V-axis side. This alternately denotes that the (H_{ult}) value of group pile can be enhanced with increasing pile spacing due to the mitigation of stress overlapping of soil in between the piles under group interaction. On the contrary, the pile spacing shows almost no effect on the (V_{ult}) value. Tangi et al. (2011) also demonstrated that the spacing of tri-pile foundation has a great influence on the ultimate horizontal bearing capacity (H_{ult}) and ultimate moment capacity (M_{ult}).

Figure 16 illustrates the normalized elliptical shape failure envelopes under ultimate states in terms of normalized loads (V/V_{ult}) and (H/H_{ult}) in *V-H* space without moment load (M/M_{ult}=0) for single and group pile. The normalized failure envelopes can be approximated using the regression equation of Eq. (1) by specifying zero moment load (M=0) and presented in the following section.

Figure 17 shows the failure envelopes under ultimate states in *V-H* space with moment load ($M/M_{ult}\neq 0$) for single pile (D=1.5 m, L=40 m) and group pile (D=1.5 m, L=40 m, S=16 m). As shown in Figs. 17(a) & (c), the envelopes contract with the increasing moment loads and theoretically become the origin of coordinate system of *V-H* space for the moment load (M/M_{ult})=1.00, namely, the moment load approaches ultimate value (M=M_{ult}). Figures 17(b) & (d) illustrate that the normalized envelopes eventually turn to be a unique elliptical

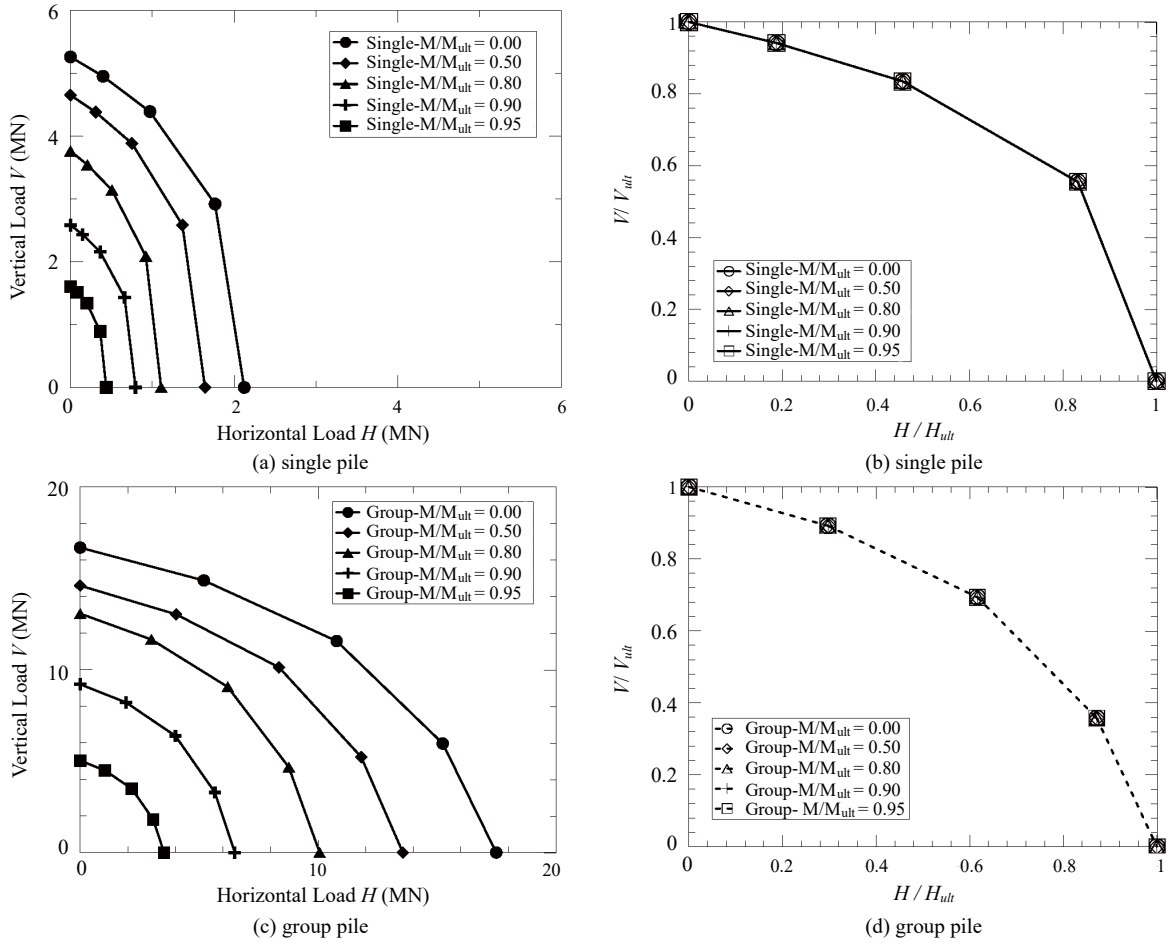

Fig. 17. ***V-H*** **envelope of bearing capacity (*V-H* envelope) and normalized *V-H* envelope under with moment load ($M/M_{ult} \neq 0$) (a) & (b) single pile and (c) & (d) group pile.**

shape curve which can be approximately fit by Eq. (1) with moment load ($M \neq 0$) and presented in the following section.

5. *V-H-M* Envelope Surface of Bearing Capacity (or Ultimate *V-H-M* Load Capacity) (*V-H-M* Envelope)

With the combination of normalized vertical, horizontal and moment loadings (V/V_{ult}, H/H_{ult}, M/M_{ult}) of the jacket foundation, 3-D failure envelopes for single and group pile can be plotted as displayed in Fig. 18. For jacket foundations of OWT in the marine soil strata of OWF at Changhua coast, the 3-D failure envelopes can be applied in the preliminary design stage to evaluate the stability and suitability of the foundations subjected to *V-H-M* combined loading. A normalized combined loading (V/V_{ult}, H/H_{ult}, M/M_{ult}) falls inside, outside or on the failure envelope representing that the foundation situates at a stable, unstable (failure state) or critical state condition respectively.

From Fig 16 and Fig 17, the normalized vertical (V/V_{ult}) and horizontal (H/H_{ult}) bearing capacity curves under different normalized moment loads (M/M_{ult}) show that these curves are similar to a Lamé curve in the first quadrant. Therefore, the normalized 3-D ultimate *V-H-M* bearing capacity envelopes (or failure envelopes in Fig. 18) for a specific moment loading (M) on pile foundation of OWT are expressed using the equation of Lamé curve in first quadrant, Eq. (1), which can be used in the scope of a preliminary design for jacket foundations in marine soil strata of OWF at Changhua coast.

$$\left(\frac{V}{V_{ult}}\right)^{I_N} + \left(\frac{H}{H_{ult}}\right)^{I_N} = 1 \tag{1}$$

where I_N =normalization index. V_{ult} =ultimate vertical bearing capacity of single and group pile, the value increases with increasing pile diameter (D) and pile length (L) for a given moment load (M). H_{ult} = the ultimate horizontal bearing capacity of single and group pile, the value increases with increasing pile diameter (D), length (L) and spacing (S) for a given moment load (M). V_{ult} can be approximated as:

$$V_{ult} = \left[V_{ult}^{ref} + I_{DV}(D-2) + I_{LV}(L-40)\right] \times \left[1-(M/M_{ult})^{I_{MV}}\right]^{\frac{1}{I_{MV}}} \tag{1a}$$

(single pile & group pile)

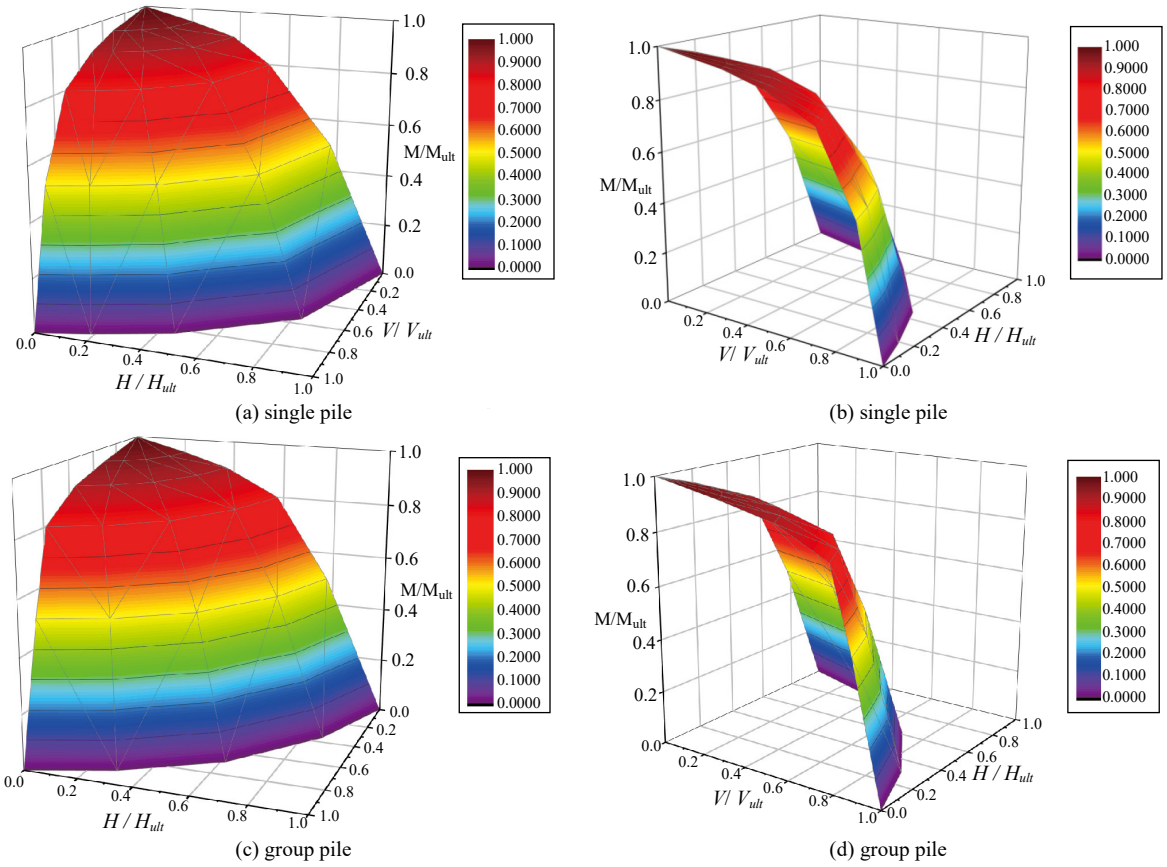

Fig. 18. Normalized *V-H-M* envelope surface of single and group pile foundation subjected to combined loading (a) & (b) front view and (c) & (d) side view after counterclockwise rotation of 75°.

Where H_{ult}^{ref} =reference value of V_{ult}. I_{DV} =pile diameter index of vertical loading. I_{LV} =pile length index of vertical loading. I_{MV} =moment index of vertical loading.

H_{ult} can be approximated as:

$$\begin{aligned} H_{ult} &= \left[H_{ult}^{ref} + I_{DH}(D-2)\right] \\ &\quad \times \left[1-(M/M_{ult})^{I_{MH}}\right]^{\frac{1}{I_{MH}}} \quad (\text{single pile}) \\ &= \begin{bmatrix} H_{ult}^{ref} + I_{DH}(D-2) + I_{LH}(L-40) \\ +I_S(S-16) \end{bmatrix} \\ &\quad \times \left[1-(M/M_{ult})^{I_{MH}}\right]^{\frac{1}{I_{MH}}} \quad (group\ pile) \end{aligned} \tag{1b}$$

where H_{ult}^{ref} = reference value of H_{ult}. I_{DH} = pile diameter index of horizontal loading. I_{LH} = pile length index of horizontal loading. I_S =pile spacing index. I_{MH}=moment index of horizontal loading. Values for different variables and indexes are listed in Table 5. The reference ultimate vertical and horizontal bearing capacity values for Single Pile and Group Pile are ultimate berating capacity of Single Pile with D = 2 m L = 40 m and Group Pile with D =2 m, L =40 m S =16 m. Other indexes in Table 5 are derived by fitting numerical simulation results (show in Fig 9, Fig 11 and Fig 13) with respect to the D, L and S of piles.

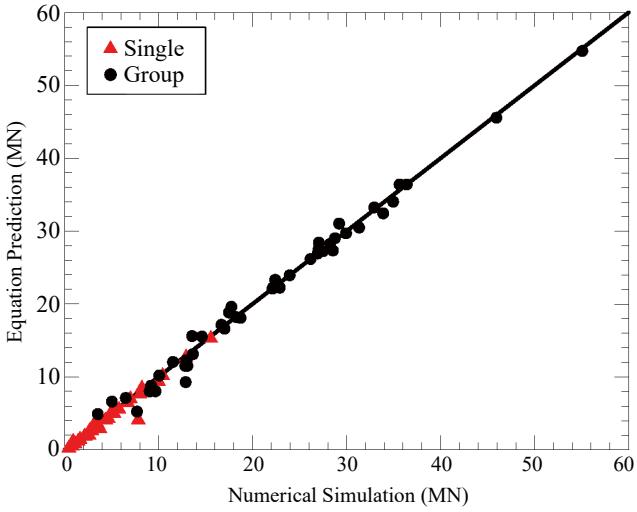

Fig.19. Comparison between prediction using Eqs. (1a) or (1b) and numerical simulation for bearing capacities (V_{ult}) and (H_{ult}) (V_{ult})=V_{ult}[D, L, (M/M_{ult})] for Eq. (1a); (H_{ult})=H_{ult}[D, L, (M/M_{ult})] for Eq. (1b).

Table 5. Variables of bearing capacity envelopes.

Variables	Single Pile	Group Pile
Normalization index, I_N	1.70	1.50
Reference ultimate vertical bearing capacity, V_{ult}^{ref}	6.708 MN (D=2 m, L=40 m)	22.233 MN (D=2 m, L=40 m, and S=16 m)
Pile diameter index of vertical loading, I_{DV}	2.925 for $L \leq$40 m 5.102 for L>40 m	10.200 for $L\leq$40 m 18.317 for L>40 m
Pile length index of vertical loading, I_{LV}	0.091 for $L\leq$40 m 0.373 for L>40 m	0.402 for $L\leq$40 m 1.417 for L>40 m
Reference ultimate horizontal bearing capacity H_{ult}^{ref}	2.865 MN	26.159 MN (D=2 m, L=40 m, and S=16 m)
Pile diameter index of horizontal loading, I_{DH}	1.45	14.667 for $D\leq$ 2 m 7.092 for D>2 m
Pile length index of horizontal loading, I_{LH}	---	0.222 for $L\leq$40 m 0.078 for L>40 m
Pile spacing index, I_S	---	1.012 for $S\leq$16 m 0.523 for S>16 m
Moment index of horizontal loading, I_{MH}	1.70	1.80

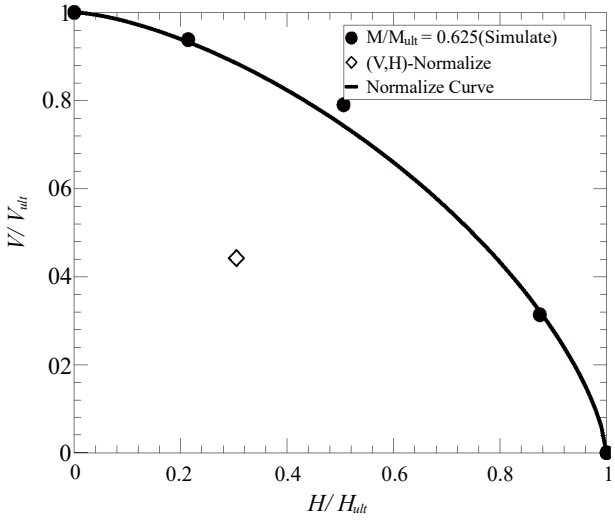

Fig. 20. Applied combined loading (*V*, *H*) and normalized *V*-*H* envelope for the stability inspection of group pile (2×2) foundation design.

For a specific moment load (M), the ultimate bearing capacities (V_{ult}) and (H_{ult}) of the jacket foundation for the given pile diameters (D) and pile lengths (L) can be predicted using regression Eqs. (1a) and (1b) respectively and compared with those from numerical simulation, as shown in Fig. 19. The excellent coincidence of the comparisons verifies the accuracy and reliability of the aforementioned regression equations. In addition, the ultimate moment load (M_{ult}) for the given pile spacing (S) can be simply determined by Fig. 13.

6. Application of *V*-*H*-*M* Envelope for Foundation Design of OWT

A procedure for inspecting the suitability and stability of jacket foundation design in marine soil strata of OWF at Changhua coast is introduced in this section. The design is based on the *V*-*H*-*M* combined loadings of V=12 MN, H=6 MN and M=250 MN-m.

(1) Determine a proper measurement and configuration of jacket foundation (D=2.0 m, L=50 m and S=20 m of 2×2 piles) which possesses an ultimate moment capacity M_{ult}=400 MN-m (> M=250 MN-m) according to Fig. 13.

(2). Calculate ultimate vertical and horizontal bearing capacities V_{ult}=30.85 MN (27.16 MN from simulation) and H_{ult}=21.26 MN (19.69 MN from simulation) using regression Eqs. (1a) and (1b) (M/M_{ult}=250/400=0.625) respectively.

(3). Substitute (V/V_{ult})=12/30.85=0.389 and (H/H_{ult}) = 6/21.26 = 0.282 into normalized ultimate *V*-*H*-*M* bearing capacity envelope Eq. (1) to obtain $[(0.389)^{1.5} + (0.282)^{1.5}]=0.392<1.0$. This denotes that the combined loading falls inside the failure envelope as illustrated in Fig. 20 and also demonstrates the jacket foundation design (D=2.0 m, L= 50 m and S=20 m of 2×2 piles) is capable of resisting the combined loading (V, H, M)=(12 MN, 6 MN, 250 MN-m) under stable situation.

VII. CONCLUSIONS

A parametric study based on numerical simulation was performed for a supporting system consisting of a jacket support structure with four-pile foundation for large OWT in deep waters installed on the marine soil strata. The marine soil strata were determined by the 19 boring logs of offshore exploration drilling at the OWF nearby Changhua coast of

Western Taiwan. The effects of pile length (L), pile diameter (D) and pile spacing (S) on the responses of the foundation were inspected in the context of ultimate bearing capacities (V_{ult}, H_{ult} and M_{ult}) under combined loadings (or V-H and V/V_{ult}~H/H_{ult}~M/M_{ult} loadings). The following conclusions can be drawn from numerical results:

(1). The distributions of lateral displacement and bending moment of tubular steel model pile from large scale lateral loading test conducted in laboratory can be well captured using Mohr-Coulomb soil model and embedded pile element.

(2). The ultimate vertical bearing capacity (V_{ult}) enhances obviously with the increases of pile diameter and pile length. Particularly, the enhancement of (V_{ult}) value turns into evident as L>40 m. The vertical loading efficiency of the pile in the group is slightly affected by the pile spacing due to overlapping of soil stressed reaction zones.

(3). The horizontal bearing capacity (H_{ult}) significantly ascends with the increase of pile diameter and pile length. The stress overlapping of the soil resisting zones for the individual piles in the group pile can be mitigated by increasing the pile spacing. As a result, the horizontal bearing capacity of group pile $(H_{ult})_{group}$ noticeably enhances with the increase of pile spacing. In addition, the bearing characteristics of the jacket foundation subjected to moment loading (M_{ult}) are similar with those subjected to horizontal loading (H_{ult}).

(4). The failure envelopes under ultimate states in terms of normalized loads (V/V_{ult}) and (H/H_{ult}) in V-H space with moment load (M/M_{ult}≠0) turn to be a unique curve of elliptical shape and can be approximated by a best fit function.

(5). With the combination of normalized vertical, horizontal and moment loadings (V/V_{ult}, H/H_{ult}, M/M_{ult}) of the jacket foundation, 3-D failure envelopes for single and group pile can be plotted and applied in the preliminary design of jacket foundations of OWT in the marine soil strata of OWF at Changhua coast to evaluate the stability and suitability of the foundations.

The 3-D ultimate bearing capacity envelope V/V_{ult}~H/H_{ult} ~M/M_{ult} can be expressed as functions of the pile diameter, pile length and pile spacing and used to design four-pile (=2×2) jacket foundations under combined loadings. Meanwhile, the mechanical stability and safety requirement of the designed foundations can be inspected with simplicity and efficiency

REFERENCES

Abdel-Rahman, K. and M. Achmus (2005). Finite element modelling of horizontally loaded monopile foundations for offshore wind energy converters in Germany. The Proceedings of the First International Symposium on Frontiers in Offshore Geotechnics (ISFOG), Perth, Australia, 19–21 September, 391–397.

Achmus, M., C. T. Akdag and K. Thieken (2013). Load-bearing behavior of suction bucket foundations in sand. Applied Ocean Research 43, 157–165.

Achmus, M., K. Abdel-Rahman and F. tom Wörden (2007). Geotechnical design of piles supporting foundation structures for offshore wind energy converters, in: J. S. Chung, S. W. Hong, S. Nagata, A.J.N.A. Sarmento, W. Koterayama (Eds.). Proceedings of the Sixteenth International Offshore and Polar Engineering Conference, International Society of Offshore and Polar Engineers (ISOPE), Lisbon, 322–327.

Akdag, C. T. (2016). Behavior of closely spaced double-pile-supported jacket foundations for offshore wind energy converters. Applied Ocean Research 58, 164-177.

Aliasger, H. and M. Gopal (2012). Three-dimensional finite element modelling of monopiles for offshore wind turbines. The 2012 world congress on Advanced in Civil, Environmental, and Materials Research (ACEM¢ 12), Seoul, Korea, August 26-30, 2012.

American Petroleum Institute (API) (2000). Recommended Practice for Planning, Designing, and Constructing Fixed Offshore Platforms-Working Stress Design. API Recommended Practice 2A-WSD (RP2A-WSD), 21st edition, Washington DC.

Bienen, B., C. Gaudin, M. J. Cassidy, L. Rausch, O. Ahmad Purwana and H. Krisdani (2012). Numerical modelling of a hybrid skirted foundation under combined loading. Computers and Geotechnics 45, 127-139.

Byrne, B.W. and G. T. Houlsby (2003). Foundations for Offshore Wind Turbines. Philosophical Transactions of the Royal Society of London, Series A 361, December, 2909-2930.

Chen, H. B. and Y. X. Zhao (2012). S77 R70MT test fan foundation design and construction. Design of Water Resources and Hydroelectric Engineering 31(1), 1-4. (in Chinese).

de Vries, W. E. and J. van der Tempel (2007). Quick Monopile Design. Proceedings, European Offshore Wind Conference, Berlin, Germany.

Duan, Y. F., H. Y. Ran, and F. L. Li (2010). Design of foundation for offshore wind field. Journal of Water Resources and Architectural Engineering 8(1), 129-131. (in Chinese)

Executive Yuan, Atomic Energy Council (2014). Development of Design Techniques of Foundation Engineering for Support Structure of Offshore Wind Turbines. Research Reports.

Haiderali, A. and G. Madabhushi (2012). Three-dimensional finite element modelling of monopiles for offshore wind turbines. The 2012 World Congress on Advances in Civil, Environmental, and Material Research (ACEM¢ 12), Seoul, Korea, August 26–30, 2012.

Hammar, L., S. Andersson and R. Rosenberg (2010). Adapting offshore wind power foundations to local environment. Swedish Environmental Protection Agency, Translated by Dimming, A., Vindval Report 6367.

International Electrotechnical Commission (IEC) (2005). Wind Turbines-Part 1: Design Requirements. International Standard: IEC 61400-1, Edition 3.0.

Jacky, J. (1944). The coefficient of earth pressure at rest. In: Hungarian (A Nyugalmi, Nyomas Tenyezoje). Journal of the Society of Hungarian Architects and Engineers Budapest, Hungry, 355-358.

Jonkman, J.M., S. Butterfield, W. Musial and G. Scott (2009). Definition of a 5-MW Reference Wind Turbine for Offshore System Development. Technical Report NREL/TP-500-38060, National Renewable Energy Laboratory, Golden, Colorado, USA.

Kim S. R., L.C. Hung and Oh M (2014). Group effect on bearing capacities of tripod bucket foundations in undrained clay, Ocean Eng. 79 (2014) 1–9.

Kourkoulis R., F. Gelagoti and A. Kaynia (2012). Seismic Response of offshore wind turbine foundations. 15th World Conference on Earthquake Engineering, Lisbon, Portugal.

Lesny, K. (2008). Foundations for offshore wind energy converters-Recommendations for concept and design. BAUTECHNIK, 85(8), 503-511.

Liu, B. X. (2009). Study on bearing capacity behavior of pile foundation for offshore wind turbines using 3-D FEM. Dalian University of Technology, China, Master Thesis. (in Chinese)

Liu, M. M., M. Yang and H. J. Wang (2014). Bearing behavior of

wide-shallow bucket foundation for offshore wind turbines in drained silty sand. Ocean Engineering 82, 169-179.

Liu, R., L. Wang, H. Y. Ding, J. J. Lian and B. R. Li (2014). Failure envelopes of large-diameter shallow buried bucket foundation in undrained saturated soft clay under combined loading conditions. Chinese Journal of Geotechnical Engineering 36(1), 146-154. (in Chinese)

Meyerhof, G. G. (1976). Bearing capacity and settlement of pile foundations. Journal of the Geotechnical Engineering Division, American Society of Civil Engineers 102(GT3), 197-228.

Ministry of The Interior, Construction and Planning Agency, Taiwan (2001). Building Infrastructure Design Specifications. (in Chinese)

Murphy, G., D. Igoe, P. Doherty and K. Gavin (2018). 3D.